Strål
säkerhets
myndigheten
Swedish Radiation Safety Authority

Author: Sofia Björnsson
Jiaxin Chen

Research

2012:02

Evaluation of activity build-up experiments

Report number: 2012:02 ISSN: 2000-0456
Available at www.stralsakerhetsmyndigheten.se

SSM perspective

Background

Nuclear power plant staff is exposed to radiation from radioactive materials in connection with for example maintenance work in the facility. Radioactive nuclides are mainly produced by neutron activation of corrosion products in construction materials passing through the reactor core.

The radioactive nuclides, essentially Co-60, are then transported with the water to other systems in the plant. There, they form metal oxides on the system components and this is called activity build-up, which contributes to radiation exposure of staff.

The activity build-up is closely related to the water chemistry environments, such as concentration of oxygen and/or iron, nickel, cobalt or other ions in the water. An experimental system has been built at Studsvik Nuclear AB to study the activity build-up as a function of different experimental parameters.

Objectives

This project aims to understand how the water chemistry affects the activity build-up on surfaces in different systems in Swedish nuclear power plants, which in turn provides information on conditions required to reduce the radiation exposure to power plant staff. The study was done to obtain knowledge about water chemistry conditions preferred to minimize the activity build-up.

A number of experiments have previously been performed at Studsvik Nuclear AB. The effects on the activity build-up from iron, nickel and zinc ions were studied. The metal oxides formed were also studied with high-resolution microscopy to provide further information on the progress of activity build-up.

The goal of this project was to assess the hitherto performed experiments to obtain a deeper understanding of the activity build-up. This was done through evaluation of how different parameters affect the activity build-up in the performed experiments.

Results and need for further research

The evaluation has identified the chemical reactions which govern the production and dissolution of the metal oxides present on the system components. These reactions are important for activity build-up and take place at the interface between the material and water. The reactions depend on the metal ions present in the water, for example iron and nickel ions increase the activity build-up, while zinc ions reduce the activity build-up. The stability of metal oxides can be correlated to the dissolution rate of the construction material.

This work has also identified the water flow rate and flow image as relevant to the activity build-up. How this affects the activity structure is not clear, but proposed to be studied in the future. A discussion of the potential impact from zinc ions on the course of activity build-up is also given in the report. Possible effects of zinc addition on activity build-up are the reduction of iron and nickel species in the water, and the formation of less amount of oxide that incorporates activity.

Project information
Contact person SSM: Charlotte Lager
Reference: SSM 2010/3544

Strål
säkerhets
myndigheten
Swedish Radiation Safety Authority

Authors: Sofia Björnsson and Jiaxin Chen
Studsvik Nuclear AB

2012:02

Evaluation of activity build-up experiments

Date: january 2012
Report number: 2012:02 **ISSN:** 2000-0456
Available at www.stralsakerhetsmyndigheten.se

This report concerns a study which has been conducted for the Swedish Radiation Safety Authority, SSM. The conclusions and viewpoints presented in the report are those of the author/authors and do not necessarily coincide with those of the SSM.

SSM 2012:02

Contents

Evaluation of activity build-up experiments

Abstract

Maintaining radioactivity low at system surfaces in BWR-plants is of importance for minimizing doses to staff working with maintenance work at the plants according to the ALARA, As Low As Reasonable Achievable, principle. The composition and microstructures of metal oxides that are formed on system piping surfaces are of great importance for the activity levels in BWR, which are in turn closely related to water chemistry environments. An experimental system has been built at Studsvik Nuclear AB to study activity build-up as a function of different experimental parameters. Up to now, the influence of different concentrations of iron, nickel and zinc species have been studied under simulated BWR-conditions.

The objective of this report is to identify parameters that may be of importance for activity build-up. This has been done through evaluation of the experimental data collected so far within the project frame. It may provide an improved understanding about the nature of various activity changes observed. It is also helpful for designing further experimental studies.

The importance of precipitation and dissolution reactions in the oxide/water interface for activity build-up has been pointed out in the report. This has been highlighted through correlation of data from activity release studies to the dissolution rate of oxide ($NiFe_2O_4$) in the oxide/water interface which in turn has been correlated to the corrosion rate of stainless steel in BWR-environments.

Utvärdering av aktivitetsupp-byggnadsexperiment

Sammanfattning

Det är av stor vikt att hålla den joniserande strålning som personal på kärnkraftverk utsätts för låg. Personal utsätts för joniserande strålning i samband med reparation och underhåll av anläggningen. Radioaktiva nuklider produceras genom neutronaktivering av korrosionsprodukter från konstruktionsmaterialen som passerar reaktorhärden. De radioaktiva nukliderna transporteras sedan med vattnet ut till de övriga systemen. Där fastnar de radioaktiva nukliderna på systemens insidor, främst Co-60, genom inkorporering i metalloxider på systemdelarna. Detta kallas för aktivitetsuppbyggnad. Det är dessa radioaktiva nuklider som ger strålning till personal vid olika reparations- och underhållsarbeten.

Aktivitetsuppbyggnaden påverkas av vattnets kemiska sammansättning, exempelvis hur mycket syre och/eller järn-, nickel-, kobolt- eller andra joner som finns i vattnet. Studsvik har byggt upp en experimentell utrustning för att kunna studera hur aktivitetsuppbyggnaden påverkas av olika parametrar i vattnet. På så sätt kan kunskap erhållas om vilka vattenkemiförhållanden som är att föredra för att minimera aktivitetsuppbyggnaden. Detta ger förut-sättningar att minimera den joniserande strålning som personal på kärnkraftverk utsätts för.

Ett antal experiment har utförts på Studsvik, där inverkan av järn- nickel- och zinkjoner på aktivitetsuppbyggnaden studerats. De bildade metalloxiderna har även utvärderats med högupplösande mikroskopi för att ge ytterligare information om förloppet. Målet med detta projekt har varit att utvärdera de hittills utförda experimenten för att erhålla en djupare förståelse för förloppet aktivitetsuppbyggnad. Detta har gjorts genom att på ett systematiskt sätt utvärdera hur olika parametrar påverkar aktivitetsuppbyggnaden i de utförda experimenten.

Utvärderingen har identifierat de kemiska reaktioner som styr uppbyggnaden och upplösningen av de metalloxider som finns på systemdelarna som betydelsefulla för aktivitetsuppbyggnaden. Dessa reaktioner äger rum i gränsskiktet mellan materialet och vattnet. Reaktionerna är beroende av vilka metalljoner som finns i vattnet, exempelvis ökar järn- och nickeljoner aktivitetsuppbyggnaden, medan zinkjoner minskar aktivitetsuppbyggnaden. Stabiliteten hos metalloxiderna kan korreleras till konstruktionsmaterialets upplösningshastighet. Arbetet har även identifierat vattnets flödeshastighet samt flödesbild som betydelsefull för aktivitetsuppbyggnaden. På vilket sätt denna påverkar aktivitetsuppbyggnaden är dock inte klarlagt, utan föreslås studeras vidare i kommande etapper. En diskussion kring zinkjonens potentiella påverkan på förloppet aktivitetsuppbyggnad ges även i rapporten.

1 Introduction

Maintaining activity build-up at a reasonably low level on BWR (boiling water reactor) system surfaces is of importance to minimize exposure dose to staff working with maintenance work at the plants according to the ALARA, As Low As Reasonable Achievable, principle. The primary nuclide of importance in this context is Co-60. Co-60 is produced primarily in fuel CRUD through neutron activation of its mother nuclide, Co-59, a species of the deposited corrosion products of structural materials. Upon interaction with reactor water, Co-60 may be released to primary water, as either dissolved ions or particulates, transported to system piping surfaces and partly incorporated into the oxide films being formed on the system surfaces. The composition and microstructure of the oxide films are of great importance for the activity levels in BWR.

At Studsvik, a series of experimental work has been carried out to study activity build-up on stainless steel 316L material under simulated BWR conditions. In particular, the role of iron, nickel and zinc species in the water in activity build-up rate has been investigated [1-4]. The experiments utilized an autoclave loop system whose hot parts were made of a titanium alloy material to minimize any severe interference by corrosion product release from the loop parts. It allowed a more precise control over the concentrations of different species of interest for parametric studies. It is of importance to point out that trends in activity build-up are studied in these experiments. The discussions given in this report are therefore preliminary and needs further validation, which is beyond the scope of this work.

To correlate the observed activity build-up with the characteristics of oxide films formed, a series of high resolution electron microscopy work on the exposed samples from the loop studies have been performed [5-6]. The implication from these electron microscopy studies is further elaborated in this report. The overall objective is to provide an improved understanding about the nature of various activity changes observed and as guidance in experimental design for further exploration of activity build-up in Swedish BWRs.

2 Objective

The objective of this report is to further evaluate the experimental data collected so far within the “activity build-up” project frame. This report could therefore be seen as a follow-up of the earlier reported work [1- 4].

The objective is to provide an improved understanding about the nature of various activity changes observed in the experiments. To realize this, the experimental data collected so far have been further analysed, evaluated and discussed regarding the following items:

1. Influence of flow velocity of water.
2. Influence of ions/ corrosion products.
3. Activity release.
4. Microstructure.

The main results from the evaluation are summarized in the report. The detailed analysis of experimental data are presented and summarized in Appendix A.

3 Background

Activity build-up has been studied in an experimental system built at Studsvik Nuclear AB. The high temperature part of the system is made of titanium alloy. A detailed description of the system can be found in Ref. [3]. Normal water chemistry (NWC) has been simulated in the experiments (Table 1). Activity build-up on 316L stainless steel tubes (inner diameter 4 mm) was monitored in situ using NaI gamma-detectors. In the tests activity build-up was monitored while simulated water with different concentrations of Fe, Ni and Zn were added to the loop system to see the activity response to the water chemistry changes. The main purpose of the experiment in each test within the scope of the project is summarized in Table 2. Data from these experiments and the results of oxide film characterization is further analysed, evaluated and discussed in the report. The data is discussed concerning the following items:

1. Influence of flow velocity of water.
2. Influence of ions/ corrosion products.
3. Activity release.
4. Microstructure.

Table 1
Experimental conditions for the activity build-up experiments.

Temperature	280 ^{o}C
Pressure	9 MPa
pH	Neutral
Conductivity	<0.2 µS/cm depending on concentrations of added ions
Linear flow velocity	0.6 m/s
Reynolds number	19 000 (= turbulent)
O_2	500 ppb
Co	0.1 ppb Co-59 ($CoSO_4$) marked with Co-60
Fe, Ni, Zn	Different concentrations, from nitrates

Table 2
Main purposes of the experiments performed in the experimental series.

Experiment/Ref	Main purpose
K104:1 [1]	To qualify the experimental system.
K104:2 part 1 [2]	To study activity build-up under Ni surplus.
K104:2 part 2 [2]	To study activity build-up for different concentrations of Fe, for example, to check if there is any pronounced effect of oxide particle deposition upon activity build-up when more Fe is injected to the system.
K104:3 [3]	To study activity build-up and its correlation with concentration ratio of [Fe] to [Ni].
K104:4 [4]	To study activity build-up and its correlation with concentration ratio of [Fe] to [Zn].

4 Evaluation of activity build-up experiments

4.1 Influence of flow velocity

The purpose of this section is to evaluate how the flow velocity of the water affects the activity build up.

In the experimental series performed up to now the flow velocity has been held constant. In one occasion however, in the conduct of one experiment, K104:2 part 1, the flow velocity of the water was accidently reduced over a short period of time. The reduced flow velocity was accompanied by a large activity increase on the piping surface, Figure 1, Appendix A.

The reduction in flow velocity has the following consequences for the experiment:

- Causes an increase in bulk concentration of ions in the water.
- Reduced flow velocity causes a thicker region close to the pipe surface where the transport of ions from the bulk solution into the surface is driven by diffusion. This implies that less ions from the bulk water reaches the pipe surface for a reduced flow velocity. Moreover species liberated at the pipe surface diffuse more slowly to the bulk water as the flow velocity is reduced.

To evaluate what kind of information concerning effects of flow velocity upon activity build-up that could be drawn from the accidental reduction of flow velocity observed in experiment K104:2 part 1 this data is further analysed in section 1.1 in Appendix A.

The result of the analysis in Appendix A indicates that the increase in ***bulk*** Ni concentration due to the reduced flow velocity is not the main reason for the increased activity build-up.

The reduced flow velocity causes a thicker diffusion layer close to the pipe surface. This implies that less Ni species from the bulk water reaches the pipe surface. As will be shown in section 4.2 the addition of Ni species to the water reduces activity build-up. The reduction of flow velocity of the water and followed lower concentration of Ni at the pipe surface would then result in an activity increase as seen in the experiment.

To study the influence of the flow velocity upon the activity build-up a systematic study is recommended where the flow velocity of the water is changed as the ***bulk*** concentration of ions is constant.

4.1.1 Literature review

The influence of flow velocity upon activity build-up has been reported in the literature by Romeo [8]. In the study activity build-up was measured on test coupons exposed for 3 years to reactor water in a test loop connected to a commercial boiling water reactor. The results show that increasing the flow velocity from 0.46 m/s (solid lines) to 6.1 m/s (dotted lines) resulted in ~50 % reduction of activity build-up for the first 5000 h of exposure (Figure 1). There are two lines for each flow rate in the figure. This corresponds to two different specimens for each flow rate located at different positions in the test loop. Consequently, the absolute value for measured activity was different depending on position in the test loop. The test coupons consisted of a Type 304 stainless steel rod with diameter 6.35 mm and the length ~330 mm that were inserted in a tube (Figure 2a). The velocity of the water in the test section was determined by the size of the annular space between the holder and the test coupon. The test coupon could be pulled out of its holder and gamma scanned when desired.

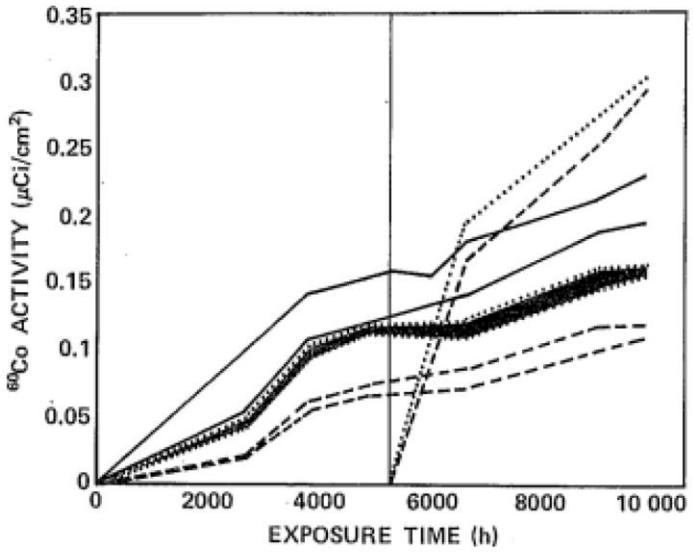

Figure 1
Activity build-up measured for different flow velocities, 0.46 m/s (solid lines) to 6.1 m/s (- - - - dotted lines) [8]. For each flow velocity (solid and dotted lines starting from t=0 h) activity build-up were measured on two different specimens located at different positions in the test loop. The set of specimens for each flow rate gave different absolute value for the measured activity.

Figure 2b show an example of the activity build-up along the test coupon. The activity build-up was not uniform across the coupon. The peak seen at the end of the scan trace corresponds to the top portion of the coupon and the location of the water outlet in the coupon holder. In this region the flow pattern changes drastically which was suggested to account for the significant change in activity distribution.

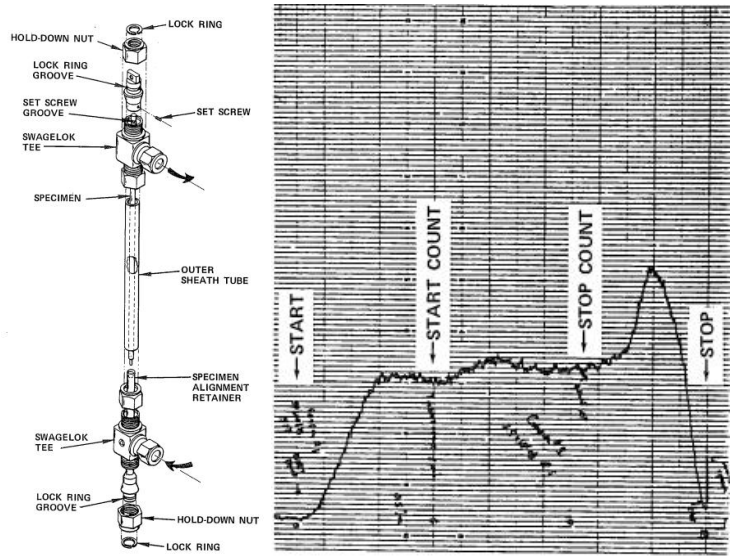

(a) (b)

Figure 2
Test coupon assembly (a) and result of gamma scan trace (b) Ref [8].

The study performed by Romeo et al shows that:

- An increased flow velocity gives lower activity build-up compared to a lower flow velocity of the water. The bulk concentration of ions (Fe, Ni etc.) in the water is not reported in the study. These parameters could be of importance for the interpretation of the effect of flow velocity.
- The flow pattern of the water is of importance for the activity build-up (Figure 2b).

4.1.2 Summary

Evaluation of the limited amount of data concerning effects of flow velocity produced in these experiments indicates that:

- The flow velocity of the water is of importance for the activity build-up since the size thickness of the diffusion layer close to the surface is affected. This influences the amount of ions that reaches the surface. The effect of flow velocity on activity build-up is consequently also dependent upon what ions and concentrations of ions that are present in the bulk water.

To evaluate the effect of flow velocity upon activity build-up a systematic study is needed where the concentration of ions in the ***bulk*** water is known and constant as the flow velocity of the water is changed. The limited data collected so far concerning effects of flow velocity on activity build-up is not enough basis to draw any conclusion on the effect of flow velocity upon activity build-up.

4.2 Influence of ions/corrosion products

The purpose of this section of the report is to evaluate in what way different ions/corrosion products affects the activity build-up.

As presented in Table 2 the influence of ions/corrosion products of Ni, Ni + Fe and Zn + Fe upon activity build-up has been studied up to now in the experimental series. A detailed analysis on the effect of Ni, Ni + Fe and Zn + Fe upon activity build-up is given in Appendix A. The result from the analysis is summarized below.

4.2.1 Chemical state of the ions/corrosion products

In studying the effect of different ions and concentrations in the water on activity build-up, we need to understand the nature of such species in the loop system. NPP reactor water may contain various kinds of species. Most commonly referred solids are Fe_2O_3, $NiFe_2O_4$ (or mixed spinel AB_2O_4 type), Fe_3O_4 and FeOOH. Most recently, the presence of amorphous CrO_2 in reactor water is also reported [9]. In addition to these solid species, a number of aqueous species including Fe(III), Ni(II) and Cr(III) are also expected. In the autoclave loop, Fe, as Fe(III) solution, is pumped directly into the location where BWR conditions persist. Before the soluble Fe(III) species reach the high temperature some chemical reactions within the injection capillary line may occur. For example, the

$$Fe(III) + O_2 \rightarrow Fe_2O_3 + FeOOH + Fe_3O_4$$

In the presence of Ni(II) the formed oxides may even be $NiFe_2O_4$ or a mixed spinel $(Ni,Fe)_3O_4$. Since these reactions in the capillary line and inside the loop line can be kinetic controlled, the kind and amount of each solid particle being formed may depend on the residence time. At present, we know neither which kinds of solid oxides being formed in the system nor the concentration of the possible soluble species over the test sections. As soon as the water is cooled to room temperature in the loop sampling lines, the cation species may not be in the same chemical form as in the high temperature water condition.

It is anticipated that solid oxides and soluble species contribute to activity build-up in different ways. When the injected solution passes the injection capillary line, some spinel (Fe_3O_4, $NiFe_2O_4$ or $(Ni,Cr,Fe)_3O_4$) grains may be formed instantly, taking up Co-60 in the water and carrying the active particles over to the test section. Some other species, such as FeOOH and Fe_2O_3 particles, may not take up Co-60 before they reach the test section. A large fraction of soluble Co-60 species is also expected to carry over the test sections.

Therefore the effect of ions or corrosion products on activity build-up to be discussed in the following sections should be elaborated within the context of our current knowledge about ions or corrosion products that are assumed to be present. In other words, when we discuss the effect of some ppb Ni^{2+}, we actually mean the effect of total nickel species, in both soluble nickel species and nickel-containing oxides that might exist over the test sections.

4.2.2 Experimental observations

The result from the detailed analysis of how different ions/corrosion products influence activity data is summarised in Figure 3. The trends for certain species are indicated with arrows in Figure 3.

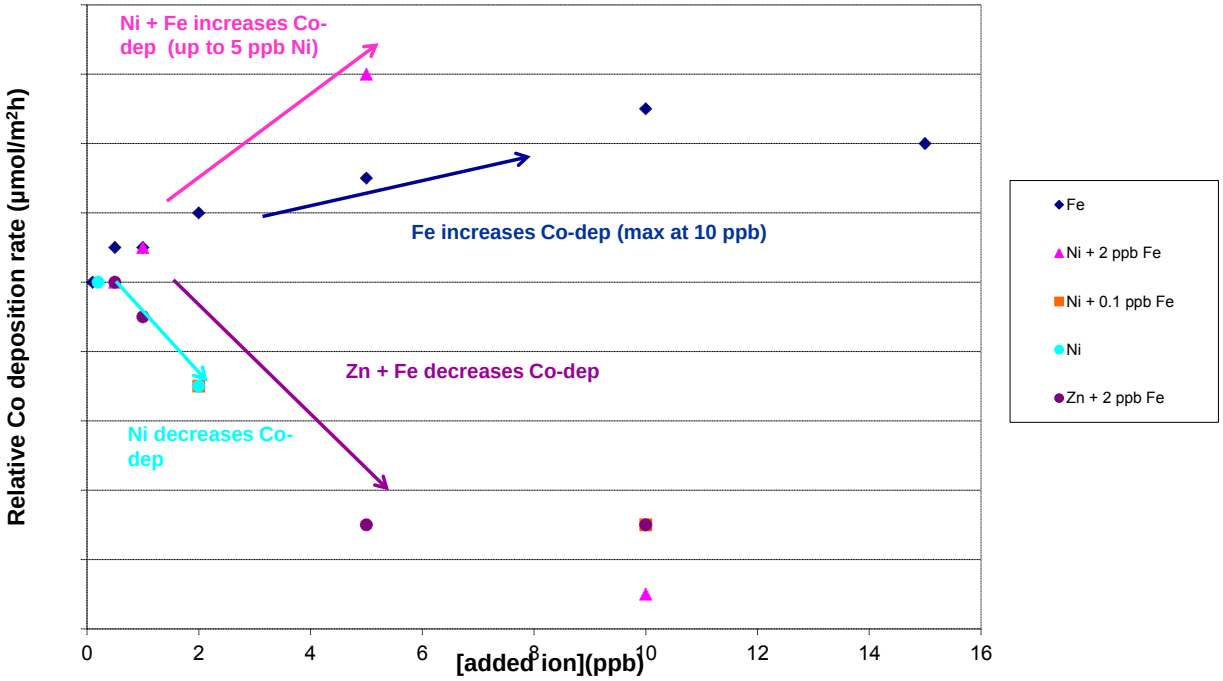

Figure 3
Co deposition rates for different species and concentration of ions in the water.

The results show that the addition of Ni and Fe (simultaneously) to the water increases the activity build-up Ni (up to 5 ppb). On contrary the addition of only Ni or the addition of mixed Zn and Fe decreases the activity build-up. The results also show that the addition of high Ni (10 ppb) and low Fe (0.1 ppb) stops activity build-up. The injection of Fe alone increases activity build-up.

In all experiments the response in activity build-up upon chemistry changes are fast (measuring time 12 h). It is also interesting to note that as soon as Zn-injection to the water is stopped the activity build-up increases immediately (S7, Figure 16 in Appendix A). These findings indicate that the processes occurring in the diffusion layer, oxide/water interface are of importance for the activity build-up.

In all experiments the influence of Ni/Ni+ Fe/Zn +Fe/ upon activity build-up has been studied in one of lines. In the other line only 0.1 ppb Co has been added in all the experiments. The activity build-up data from this line is analyzed separately in section 1.2 in Appendix A. A Co-deposition rate has been calculated. From the Co-deposition rate a rough estimation of atomic percent of Co in the outer layer of the oxide is calculated assuming the outer oxide is $NiFe_2O_4$ and the Co-atoms are evenly distributed in an oxide thickness of 0.6 μm. The atomic percent of Co is then calculated to 0.15 % for an exposure time of 1500 h.

4.2.3 Summary

The influence of ions/corrosion products of Ni, Ni + Fe and Zn + Fe upon activity build-up have been summarized in this section of the report. An overview of the results is given in Figure 3. The main features are:

- Addition of Ni and Fe (simultaneously) increases the activity build-up (up to 5 ppb Ni).
- Addition of Ni separately or injection of mixed Zn and Fe decreases the activity build-up.
- High Ni (10 ppb) and low Fe (0.1 ppb) stops activity build-up.
- Injection of high Ni (10 ppb) and Fe (2 ppb) minimizes activity build-up.
- Injection of Fe alone increases activity build-up.
- As soon as Zn-injection is stopped, activity build-up is increased.

The processes occurring in the oxide/water interface and diffusion layer are indicated to be of importance for the activity build-up.

4.3 Activity release studies

In this section of the report Co-release data from the experimental studies are further analyzed. The purpose is to receive more information about important processes for activity build-up.

4.3.1 Experimental observations

In the activity release studies the release of activity was followed as the Co injection to the water was stopped. The injection of other metal cations was kept unchanged during the release studies. The relative Co-release for different chemistries is summarized to the right of the vertical line in Figure 4.

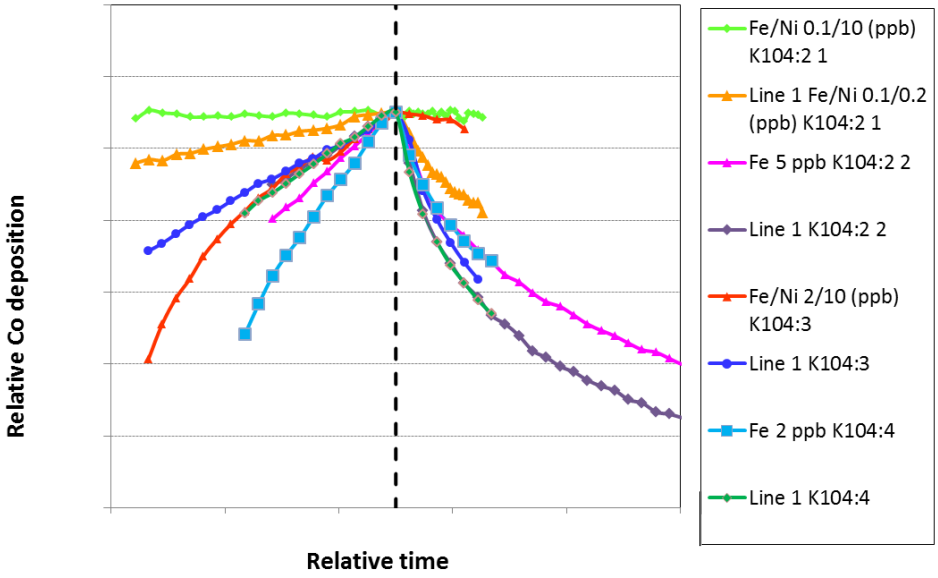

Figure 4
Release studies in all experiments on relative y- and x-axis. At the black vertical dotted line the addition of Co to the water is stopped but the addition of other ions is kept.

The following observations are made (Figure 4):

- The release of Co is lowest at a mixed injection of 10 ppb Ni and 0.1 ppb Fe (light green line).
- The release of Co is the highest for pure water (no ions added) (violet, dark green and cornflower blue).
- The release of Co is lower for injection of Fe (2 and 5 ppb), (pink and light blue) compared to the release for pure water.
- The release of Co is relatively low for the injection of a mixed Fe (0.1 ppb) and Ni (0.2 ppb) (orange) compared to the release for pure water.

4.3.2 Discussion

To get more information about important processes occurring at the oxide/water interface some rough calculations are made from the experimental data (presented in Appendix A).

Different interpretations of the Co-release data are presented and discussed in section 1.3 in Appendix A. The main results from the discussion in Appendix A are summarized below.

One assumption is made where the measured Co-release is assumed to origin from dissolution of Co-containing $NiFe_2O_4$. To validate the assumption a dissolution rate of $NiFe_2O_4$ is calculated from the experimental measured Co-release rates.

From the Co-release data a $NiFe_2O_4$ dissolution rate in the size of 10^{10} kg/m^{2}s is calculated. The calculated $NiFe_2O_4$ dissolution rate is compared with earlier reported dissolution rates for $NiFe_2O_4$ which are 3-9 x 10^{-9} kg/m^{2}s at 80 - 250 ºC [10]. The calculated $NiFe_2O_4$ dissolution rate from the Co-release data agrees well with the reported $NiFe_2O_4$ dissolution rate which indicates that the interpretation of the observed Co-release in Figure 4 as the dissolution of Co-containing $NiFe_2O_4$ in the oxide/water interface is relevant. Moreover the earlier noticed indications that the precipitation and dissolution reactions at the oxide/water interface are of importance for the activity build-up and release process are strengthened.

The importance of precipitation and dissolution reactions at the oxide/water interface is also strengthened through the observation in Figure 4 that:

- Presense of Fe and Ni in the water minimizes the Co-release of Co → the presence of Fe and Ni in the water supress the dissolution of $NiFe_2O_4$ through favoring precipitation of $NiFe_2O_4$.
- The release of Co is highest where no Fe and Ni are present in the water → No injection of Fe and Ni to the water gives the highest dissolution of $NiFe_2O_4$.

The calculated dissolution rate of $NiFe_2O_4$ (10^{-10} kg/m^{2}s) from the Co-release data could moreover be correlated to the corrosion rate of stainless steel. Assume the liberated Ni in the dissolution process of $NiFe_2O_4$ at the oxide/water interface origin from the base metal, stainless steel. Then a corrosion rate of stainless steel could be calculated from the dissolution rate of $NiFe_2O_4$ and the Ni content in stainless steel. This has been done within the scope if this project. The calculated corrosion rate of stainless steel 316L from the experimental data gives a corrosion rate of 1 µm/year. The calculated metal corrosion rate of 1 µm/year agrees very well with assumed corrosion rates for stainless steel in BWR environments. This strengthens the importance of precipitation and dissolution reactions of $NiFe_2O_4$ for the observed Co-release and the corrosion rate of the base metal. The satisfying agreement of the correlation of the dissolution rate of $NiFe_2O_4$ to the

corrosion rate of stainless steel in BWR environments validates the importance of the solubility of the oxide in contact with water for the corrosion of stainless steel in high temperature water.

An alternative way of interpretation of the Co-release data presented in Appendix A is diffusion of Co-60 through the porous inner oxide layer. This way of interpretation has not been qualified in the quantitatively in the evaluation.

4.3.3 Summary

Evaluation of activity release data show that the activity release could be correlated to the dissolution rate of the oxide in contact with the water. This indicates that the precipitation and dissolution reactions continuously going on in the oxide-water interface are of importance for the activity build-up. The calculated dissolution rate could moreover be correlated to the corrosion rate for stainless steel in BWR environments. This implies that the corrosion rate for stainless steel in BWR environments is controlled by the stability of the oxide in the oxide-water interface. The importance of precipitation and dissolution reactions in the oxide water interface has been pointed out through:

- The calculated value of oxide dissolution in the oxide/water interface (10^{-10} kg/m^{2}s), assuming the oxide is $NiFe_2O_4$, which could be further correlated to the corrosion rate of stainless steel (1µm/year).
- The presence of Fe and Ni that minimizes the release of Co → the presence of Fe and Ni in the water, due to injection, supress the dissolution of $NiFe_2O_4$.
- The release of Co is highest where no Fe and Ni are present in the water → No injection of Fe and Ni to the water gives the highest dissolution of $NiFe_2O_4$.

An alternative way of interpretation of the Co-release data is also discussed in Appendix A. This concerns the diffusion of Co-60 through the porous inner oxide layer. This way of interpretation has however not been qualified quantitatively.

4.4 Microstructure

Corroded samples from the experimental series have been characterized using high resolution scanning electron microscopy (HR SEM) and transmissions electron microscopy (HR TEM). Detailed information from the characterization is reported separately in Ref. [5-6]. One oxide sample exposed for three years in a loop connected to an operating BWR-plant exposed to NWC has also been analyzed. The evaluation from this work is reported separately in [11]. The main oxide characteristics are summarized in section 4.4.1 below. Table 3 summaries the samples that have been analyzed using TEM. In next section some examples from the microscopy evaluation is shown (pre-oxidized sample, samples from K104:2 and K104:3).

Table 3
Summary of TEM analyzed samples.

From experimental series	Pcs of samples	Samples exposed until sequence	Reference
Pre-oxidized sample	1	-	[5]
Ni surplus, K104:2	1	S6	[5]
Different ratios of Fe/Ni, K104:3	2	S3, S7	[6]
Different ratios of Fe/Zn, K104:4	7	S1, S2, S3, S4, S5, S6, S8	[6]
3 years exposure to NWC at Oskarshamn 3	1		[1]

4.4.1 Experimental observations

In this section some examples from the microscopy evaluation is shown (pre-oxidized sample, samples from K104:2 and K104:3).

In Table 4 analyze data from four samples indicated A (pre-oxidized), B (K104:2), C (K104:3) and D (K104:3) are summarized. The thicknesses of the inner oxide and inner + outer oxide layer are shown versus experimental time in Figure 5. Scanning electron microscopy (SEM) and TEM images for sample A, B, C and D are shown in Figures 6 and 7.

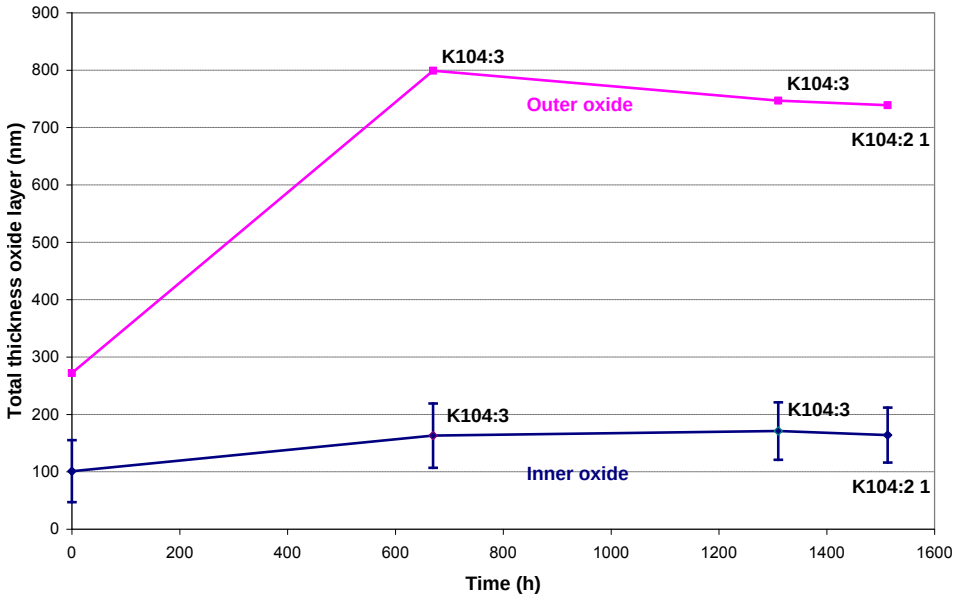

Figure 5
Total thickness (inner oxide + outer oxide) for samples A (pre-oxidized), B (K104:2), C (K104:3, S3) and D (K104:3, S7).

Table 4
Composition and thickness of inner and outer oxide layers for samples indicated A, B, C and D.

Exp/ Sample	Thickness of inner oxide layer (nm)	Chemical formulas of inner oxide layer	Grain size of outer oxide (nm)	Chemical formulas for outer oxide grains
A (pre-ox)	101±54	$Cr_{1.0}Ni_{0.4}Fe_{1.6}O_4$	171	$NiFe_2O_4/Cr_{(0-0.6)}Fe_{(2.4-3)}O_4$
B K104:2	164±56	$Cr_{0.6}Ni_{0.7}Fe_{1.7}O_4$	575	$NiFe_2O_4$
C K104:3 S3	163±50	$Cr_{0.6}Ni_{0.5}Fe_{1.9}O_4$	636	$NiFe_2O_4$ and $(Cr_xFe_y)_3O_4$ x=0-0.25 y=0.75-1
D K104:3 S7	171±48	$Cr_{0.4}Ni_{0.7}Fe_{1.9}O_4$	576	$NiFe_2O_4$ and $Ni_{0.7}Fe_{1.2}Cr_{0.1}O_3$

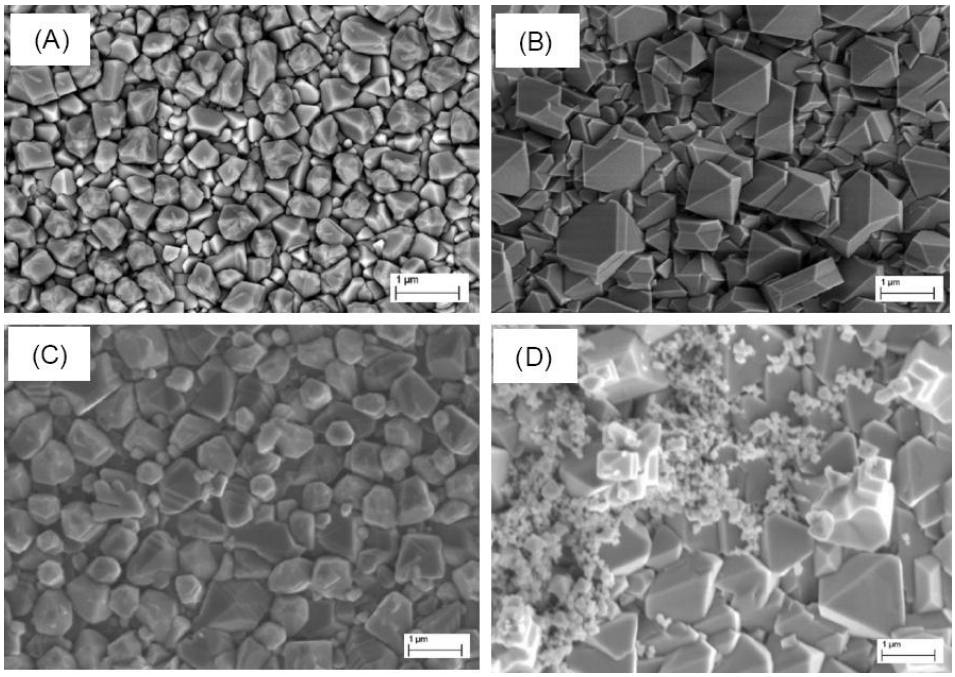

Figure 6
SEM images of the surfaces for sample A, B, C and D.

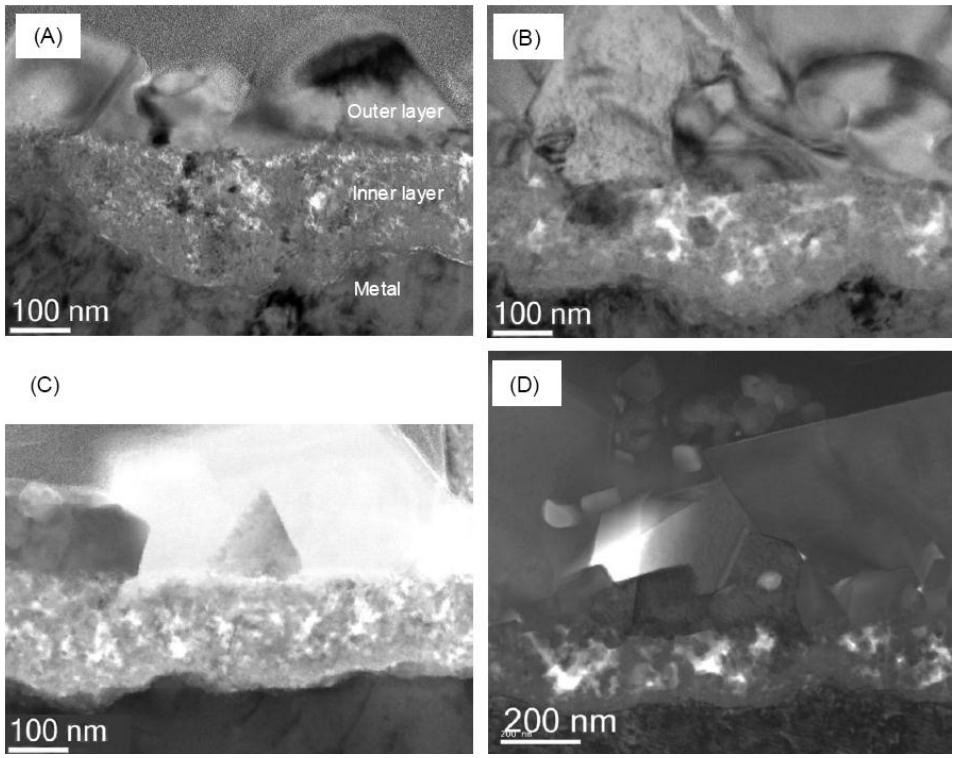

Figure 7
TEM bright field (BF) images of the cross section microstructures of samples A, B, C and D.

Assuming a constant Co-deposition rate of 0.1 μmol m^{-2} h^{-1} for an exposure period of 1500 h, the total atomic fraction of Co would be approx. 0.15 at % in a $NiFe_2O_4$ layer of 0.6 μm, which is close to the detection limit of EDX measurement in SEM or TEM. In all previous EDX measurements no trace of Co was ever detected on the exposed surfaces, not even for oxides from K104:3 test where about 0.3 % Co would have been present in the oxides. Figure 8 shows the crystal structure of $NiFe_2O_4$. $NiFe_2O_4$ is an inverse spinel, so is $CoFe_2O_4$. In other words, all Co atoms that are incorporated into the structure will occupy the octahedral coordination sites.

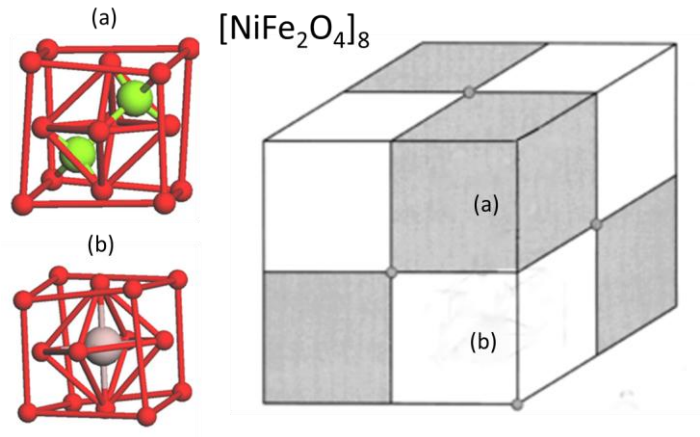

Figure 8
Crystal Structure of $NiFe_2O_4$ where Ni and Fe atoms occupy 50 % of all octahedral coordination sites (grey ball) each, another 50 % Fe atoms take all tetrahedral coordination sites (green balls).

4.4.2 Summary

In this section the main characteristics from the microcopy evaluation presented in [4-5] and [11] are summarized. A schematic summary of the main findings are presented in Figure 9.

- All K104 test samples have a dense 30 nm barrier layer consisting of epitaxial layer rich in Fe. This layer has a higher Cr content and lower Ni content than the inner oxide.
- All K104 test samples have an extensively porous inner oxide layer consisting of epitaxial layer rich in Fe. The thickness is ~160 nm and ~100 nm for the pre oxidized sample.
- Many seemingly large outer oxide grains consist of relatively small oxide grains that have merged together.

- With high Ni dosage (10 ppb) outer oxide grains are $NiFe_2O_4$. The crystals have sharp and regular edges with smooth facets. With a relatively low Ni dosage and/or mixed dosage of low concentration Fe and Ni species, two kinds of spinel, $NiFe_2O_4$ and $(Fe,Cr)_3O_4$ are formed. Oxides formed during pre-oxidation also contain two kinds of spinel phases: $NiFe_2O_4$ and $(Fe,Cr)_3O_4$.
- The thickness of the outer layer is ~600 nm for all samples except the sample formed during pre-oxidation that is ~170 nm.
- Under zinc injection, Zn is detected in the inner oxide layer, but not in the outer layer.
- The evaluated samples (in total 11 pcs where one of the samples was exposed for three years) show that the total oxide thickness is constant (~ 1 µm) after 600 h exposure.
- After pre-exposure it is mainly the outer oxide layer that increases in thickness
- The sample exposed at Oskarshamn 3 for 3 years show the same main characteristics as the samples exposed in the experimental autoclave loop system

It must be pointed out that the summary given above is the result of analysis on a limited number samples. To validate the above observation further samples and studies are needed. The results could however serve as a guide for further discussions and preliminary assumptions that need to be further validated.

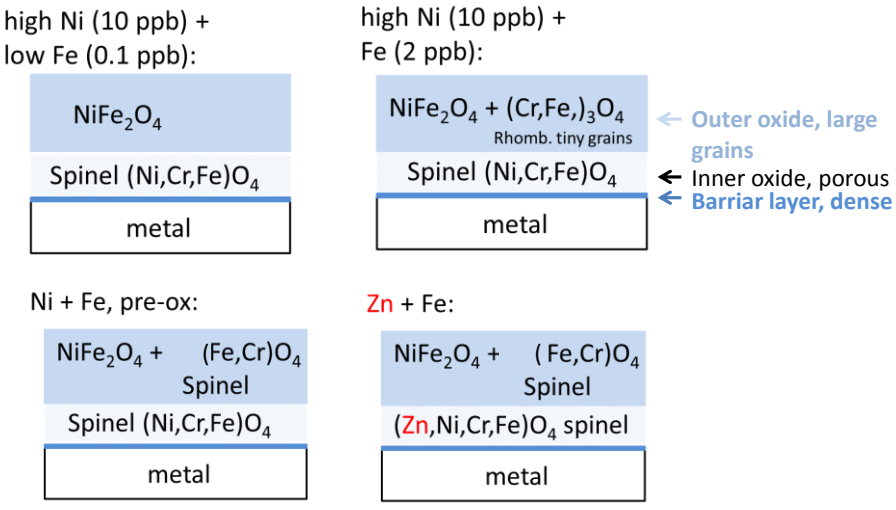

Figure 9
Schematic summary of the main characteristics from the microscopy evaluations of oxides.

5 Discussion

The importance of precipitation and dissolution reactions in the oxide/water interface has been highlighted in the report through correlation of the dissolution rate of $NiFe_2O_4$ in the oxide/water interface to the measured Co-release and corrosion rate of stainless steel.

Reduced activity build-up is observed for Zn addition. Suppose the result of Zn addition is an oxide that is more stable with respect to dissolution. According to the discussion above the result of that would be suppressed material corrosion.

This discussion supports the theory that zinc injection can suppress material corrosion leading to a general reduction of fuel CRUD deposition and therefore much reduced concentration of radionuclides in reactor water. This effect - reduced concentration of radionuclides - is however not studied in the experimental system since the Co concentration is independent of the material corrosion. This indicates that suppression of material corrosion due to zinc injection leading to a general reduction of fuel CRUD deposition and therefore much reduced concentration of radionuclides in reactor water would in that case not be the only reason for the reduced activity build-up during Zn addition.

An oxide that supresses material corrosion would, however reduce the concentration of corrosion products in the water. It has been seen in these experiments that increased concentrations of corrosion products from stainless steel (Fe and Ni) increases the activity build-up. This indicates that the effect of Zn on activity build-up could be decreased concentrations of corrosion products from stainless steel (Fe and Ni).

Followed a hypothetical discussion on the effect of Zn on activity build-up is given. The discussion is based on the nature of the precipitation and dissolution reactions continuously going on in the oxide/water interface. Through the correlation of the dissolution rate of the oxide in the oxide/water interface to the Co-release data in this work these reactions are assumed to be of importance for the activity build-up. The discussion is based on the hypothetical assumption that the precipitation of inverse spinel is favoured towards the precipitation of normal spinel upon an already existing inverse spinel oxide surface. The difference between normal and inverse spinel is the distribution of 2+ and 3+ ions in the tetrahedral and octahedral positions in the spinel structure i.e. the distribution of charge in the structures. The discussion is based on an arbitrary, but not unrealistic, assumption that precipitation of spinel with identical distribution of charge in the structure is favoured on an oxide surface towards a spinel with different distribution of charge.

The addition of Fe **and** Ni (up to 5 ppb) in the water increases activity build-up. This could be interpreted as the oxides formed at the surface during the combined addition of Ni and Fe results in a high Co deposition. According to Pourbaix-diagram for iron species in the Fe-Cr-Ni-Zn system at 285 ^{o}C presented in Figure 10, $NiFe_2O_4$ is the thermodynamic most stable phase during NWC conditions [12]. Ni and Fe added to the water give possibilities

to the formation of $NiFe_2O_4$ that could incorporate Co in a solid solution. $NiFe_2O_4$ crystallises in the inverse spinel structure which means that the Ni^{2+} ion occupies the octahedral site in the structure and the Fe^{3+} ions occupy the rest of the octahedral sites and the tetrahedral sites. In the spinel structure the occupancy of the octahedral and tetrahedral sites respectively depends upon the preference that each ion has for the different sites. The preference for a specific geometry is dependent upon the crystal field stabilization energy for that ion in the specific geometry. The crystal field stabilization energy is the result of the most favourable placement of the outer electrons in the orbitals of the ion. The site preference for a specific ion in a specific geometric environment for the combination of the ions in an oxide is reflected in the free energy of formation, ΔG, for the specific oxide. For example the Zn^{2+} ion has a high preference for tetrahedral geometry and Cr^{3+} a high preference for octahedral geometry which gives a low ΔG for formation of $ZnCr_2O_4$. ($ZnCr_2O_4$ crystallises in normal spinel structure with Zn^{2+} in the tetrahedral sites and Cr^{3+} in the octahedral sites.)

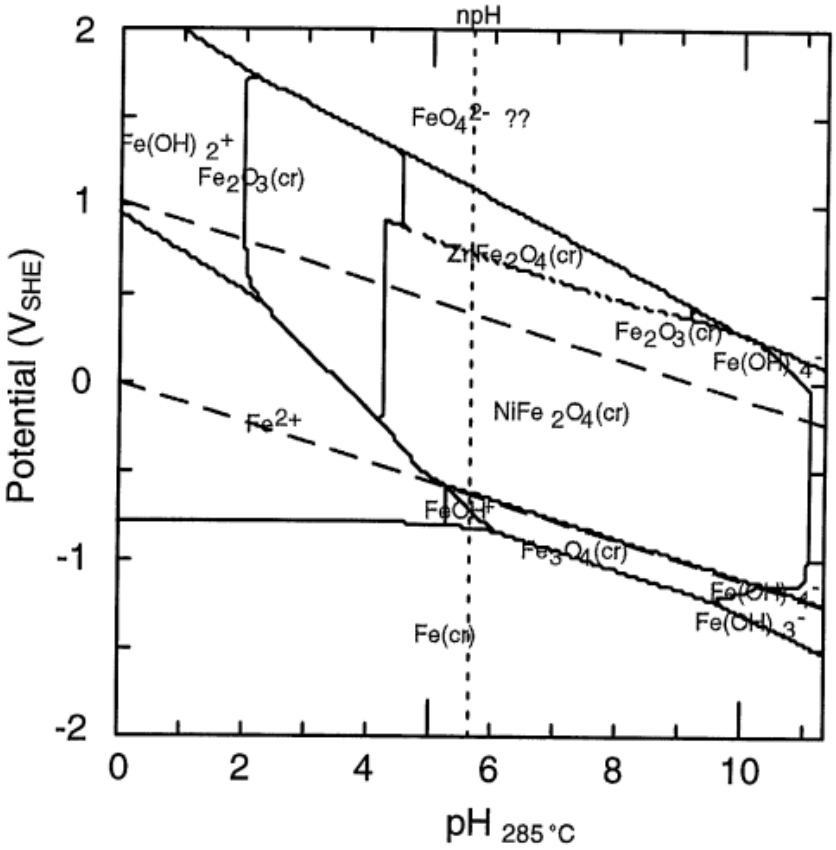

Figure 10
Pourbaix-diagram for iron species i the Fe-Cr-Ni-Zn system at 285 ^{o}C and [Fe(aq)]tot=[Cr(aq)]tot= [Ni(aq)]tot=[Zn(aq)]tot = 10^{-6} molal [12].

The experiments performed in this experimental series also show that the combined addition of Zn and Fe gives reduced activity build-up. Starting from 2 ppb Fe and in coming sequences adding increasing amounts of Zn (0.5, 1, 5, 10 ppb) significantly decreases activity build-up. Fe and Zn in the water decrease the rate for Co-deposition. This could be interpreted like as the oxides formed at the surface during the combined addition of Zn and Fe results in a lower Co deposition compared to the situation where only Fe or Ni and Fe were added to the water.

Assume the possibility to formation of $NiFe_2O_4$ is one main parameter for the activity build-up since the addition of Fe and Ni ions to the water increases the activity build-up notably. $NiFe_2O_4$ (trevorite) is an inverse spinel (Table 5) and so are Fe_3O_4 (magnetite), γ-Fe_2O_3 (maghemite) and $CoFe_2O_4$ (coferrite). According to high resolution electron microscopy characterization the dominating oxide in the outer oxide layer is an inverse spinel. The Co^{2+} fits in the inverse spinel structure of $NiFe_2O_4$. Spinels are known for forming solid-solutions with ions of similar size, like the Co^{2+} and the Ni^{2+} ion. $CoFe_2O_4$ and $NiFe_2O$ both have the inverse crystal structure where Co^{2+} and the Ni^{2+} ion have preference for octahedral geometry. Assume the presence of an inverse spinel at the outer oxide layer favour activity build-up since a solid solution inverse spinel of $[Fe^{III}]_{tetr}[(Ni,Co,Fe)^{II}]_{okt}[Fe^{III}]_{okt}O_4$ could be formed.

Table 5
Distribution of metal ions in certain oxides with classification.

Spinel		Distribution of metal ions	Classification
Magnetite	Fe_3O_4	$[Fe^{3+}]_{tetr}[Fe^{2+}Fe^{3+}]_{oct}O_4$	Invers
Trevorite	$NiFe_2O_4$	$[Fe^{3+}]_{tetr}[Ni^{2+}Fe^{3+}]_{oct}O_4$	Invers
Coferrite	$CoFe_2O_4$	$[Fe^{3+}]_{tetr}[Co^{2+}Fe^{3+}]_{oct}O_4$	Invers
Maghemite	γ -Fe_2O_3	$[Fe^{3+}]_{tetr}$ $[\square$ $Fe^{3+}]_{oct}O_3$	Invers
Franklinite	$ZnFe_2O_4$	$[Zn^{2+}]_{tetr}[Fe^{3+}Fe^{3+}]_{oct}O_4$	Normal

The $ZnFe_2O_4$ (franklinite) however, has a normal spinel structure, $[Zn^{II}]_{tetr}[Fe^{III}, Fe^{III}]_{okt}O_4$ and according to thermodynamic also a low ΔG. According to ref [13], ΔG for $ZnFe_2O_4$ is of similar size as ΔG for $NiFe_2O_4$.

Assume Zn ions are added to the water and approaching the outer oxide surface consisting mostly of spinels with the inverse spinel structure. Zn "wants" to form normal spinel at the surface, and has a driving force thermodynamically, to do this. The driving force of Zn to form normal spinel at the surface "disturbs" the formation process of the inverse spinel continuously going on in precipitation and dissolution processes at the surface. The "disturbance" effect of Zn at the oxide surface results in a smaller amount of inverse spinel ($NiFe_2O_4$) being reformed in precipitation and dissolution processes at the surface.

The consequence of this would be that less Co is incorporated in the outer oxide at the surface oxide, since less inverse spinel oxide is formed. High resolution electron microscopy studies of samples produced in this project show that the outer oxide layer does not contain any Zn. Normal spinel ($ZnFe_2O_4$) is not formed in the continuously precipitation- dissolution process going at the inverse spinel ($NiFe_2O_4$) surface. This would be true if the hypothetical assumption that formation of inverse spinel $NiFe_2O_4$ on the already existing $NiFe_2O_4$ at the surface is more favourable than the formation of normal $ZnFe_2O_4$ on the existing $NiFe_2O_4$ is true. Zn addition "disturbs" the $NiFe_2O_4$ formation resulting in less $NiFe_2O_4$ reprecipitated, therefore less Co is incorporated in the surface oxide. At high Zn additions no or minor inverse spinel manages to be reformed and the Co incorporation, activity build-up stops. As has been pointed out this "mechanism" is however of hypothetical nature and has not been validated.

Reported experimental investigations in literature show that Zn addition results in a notably thinner oxide layer [14, 15] which would support the above suggested hypothetical mechanism of Zn.

The results within this experimental series show that activity build-up increases relatively after Zn-addition. Comparing activity build-up before and after Zn addition a higher activity build-up is shown after Zn addition. Assume a certain oxide thickness is adjusted for certain chemistry and assume a relative thinner oxide is adjusted for Zn addition compared to the thickness without Zn addition that is thicker. Hypothetically a relative thinner oxide is adjusting during Zn addition. Stopping Zn addition and continuing with addition of 2 ppb Fe a relatively thicker oxide would adjust resulting in a higher activity build-up immediately after Zn addition. According to this discussion the relatively higher activity build-up observed immediately after Zn addition is returned to "normal" activity build-up as the adjusted thickness for chemistry without Zn addition is reached.

In the experimental series the response of certain chemistry, addition of ions, upon activity build-up is relatively fast (measuring time is 12 h). This strengthens the importance of precipitation and dissolution reactions for activity build-up. The reactions occurring at the interface are adjusting according to the chemistry in the water.

6 Summary

In this work series of activity build-up experiments and related high resolution electron microscopy studies have been further evaluated. The scope of the work was to identify parameters and courses that may be of importance for activity build-up on system surfaces.

The importance of *precipitation and dissolution reactions* in the oxide/water interface *for activity build-up* has been pointed out in the report.

The importance of precipitation and dissolution reactions in the oxide/water interface for activity build-up is supported by:

- The correlation of the measured activity release to the dissolution rate of $NiFe_2O_4$ at the oxide-water interface. The dissolution rate could furthermore be correlated to the corrosion rate of stainless steel in BWR-environments.
- The fast responses of changes of species in the water phase upon activity build-up (12 h).

Two possible effects of Zn addition on activity build-up are discussed in the report:

- The reduction of Fe and Ni species in the water as a result of a more stable oxide with respect to dissolution as Zn is to the water.
- The formation of less amount of oxide that incorporates activity, Co, as Zn is added to the water.

6.1 Further studies

The influence of the following parameters is suggested to be studied experimentally to gain further knowledge of the dissolution and precipitation processes identified to be of importance for the activity build-up process:

- The influence of changes in flow pattern/ velocity of the water at the sample upon activity build-up for different chemistries*.
- The release pattern for Co as Co-addition to the water is stopped for different chemistries.

*Fe+ Ni, Fe+ Zn, Fe+ Ni+ Zn

7 Acknowledgements

Financial support is gratefully acknowledged by Strålsäkerhetsmyndigheten, SSM. Karin Fritioff is especially acknowledged as contact person for this work.

PGK, Programgruppen för kemi, is gratefully acknowledged for providing data to this evaluation. Johan Lejon, OKG AB and Göran Granath, Ringhals, are gratefully acknowledged for discussions and as contact persons for projects providing as basis for this work.

Present and past colleagues at Studsvik Nuclear AB are gratefully acknowledged for scientific discussions and technical skillfulness: Hans-Peter Hermansson, Anders Molander, Charlotta Gustafsson, Stefan Forsberg, Riitta Johansson, Anders Pettersson, Per S Ekberg, Peter Gillén, Timo Jokinen, Jari Syrjänen, Gustav Pettersson, Eva Ögren, Catharina Carlsson and Camilla Berglund.

8 References

[1] Forsberg, S., Björnsson, S. & Johansson, R. (2007). *Systemytors upptag av Co-60 i närvaro av andra metalljoner*. Studsvik Nuclear AB, STUDSVIK/N-07-134.

[2] Forsberg, S. & Johansson, R. (2008). *Systemytors upptag av Co-60 i närvaro av andra metalljoner. Etapp 2 — Inverkan av nickel och järn.* Studsvik Nuclear AB, STUDSVIK/N-08-129.

[3] Forsberg, S. & Pettersson, A. (2009). *Systemytors upptag av Co-60 i närvaro av andra metalljoner. Etapp 3 — Inverkan av olika kvoter järn/nickel.* Studsvik Nuclear AB, STUDSVIK/N-09-157.

[4] Björnsson, S., Gustafsson, C. & Johansson, R. (2010). *Systemytors upptag av Co-60 i närvaro av andra metalljoner. Etapp 4 — Inverkan av olika kvoter järn/zink.* Studsvik Nuclear AB, STUDSVIK/N-10-150.

[5] Chen. J. (2010). *High resolution electron microscopy study on the thin layers formed on type 316L stainless steel under simulated BWR conditions.* Studsvik Nuclear AB, STUDSVIK/N-10-038.

[6] Chen. J. (2011). *In manuscript*, Studsvik Nuclear AB.

[7] Chen. J. (2009). *Understanding radioactivity up-take on system piping surfaces through laboratory deposition simulation.* Studsvik Nuclear AB, STUDSVIK/N-08/213.

[8] Romeo, G. (1983). *Oxidation and Radiation Buildup on Stainless Steel Components of Boiling Water Reactors,* Nuclear Technology, 63, p.110- 120.

[9] Chen, J. & Gustafsson C. "Characterization of waterborne CRUD particles from a Swedish BWR", Studsvik Report. To be issued.

[10] Chen, J. (2001). *Stability of trevorite in high temperature water, a radiotracer study*, Studsvik Nuclear AB, STUDSVIK/N(K)-01/022.

[11] Chen. J. (2011). *In manuscript*, Studsvik Nuclear AB.

[12] Beverskog, B. (1997). *Kobolt- och zinkinnehållande faser I BWR-miljö*, Studsvik Material, STUDSVIK/M-97/83.

[13] Kubaschewski, Alcock & Spencer. (1993). *Materials Thermo-Chemistry*, 6th edition Pergamon Press, New York.

[14] Hosokawa, H. & Nagase, M. (2004). *"Investigation of Cobalt Deposition Behavior with Zinc Injection on Stainless Steel under BWR Conditions"*. J. Nucl. Sci. Technol., 41, p. 682-89.

[15] Lin, C. C., (2009) *A Review of Corrosion Product Transport and Radiation Field Buildup in Boiling Water Reactors*, Progress in Nuclear Energy, 51, 207-224.

[16] Lin, C. C. & Smith, F. R., (1988), *BWR Cobalt Deposition Studies: Final report*, EPRI report. EPRI, NP-5808.

1 Detailed evaluation of activity build-up experiments

In this Appendix the experimental data are presented, discussed and evaluated. The results from the evaluation are presented in the report.

1.1 Influence of flow velocity

In this section a detailed analysis of the reduction of the flow velocity observed in K104:2 part 1 is given [2].

1.1.1 Experimental observations

In Figure 1 the activity build-up on the piping surface under 6 different concentration ratios of [Fe] to [Ni] in the red curve (line 2), is shown. In Table 1 the exposure duration at each concentration ratio and ion concentration are presented. The blue curve (line 1) shows the activity build-up when only Co was added to the water. In Sequence 3 the flow velocity of the water was accidently reduced from 20 l/h to 17 l/h for about 350 h, beginning at a time of 387 h from the first experimental sequence. During this period the activity build-up proceeds with a higher rate.

The reason behind the observation may be complex and probably difficult to explain. The flow rate reduction of the main flow was accompanied by an increase in the concentrations of the injected metal species since the injection rates of the metal species are independent upon the main flow. Reynolds number is also affected by the change in flow velocity at the sample. Being converted to Reynolds number the flow velocity change corresponds to Re 19 000 (20 l/h) and 16 000 (17 l/h). A flow under Re 2300 is laminar and above Re 2300 it is turbulent. Therefore, the reduced flow in the experiment is still turbulent.

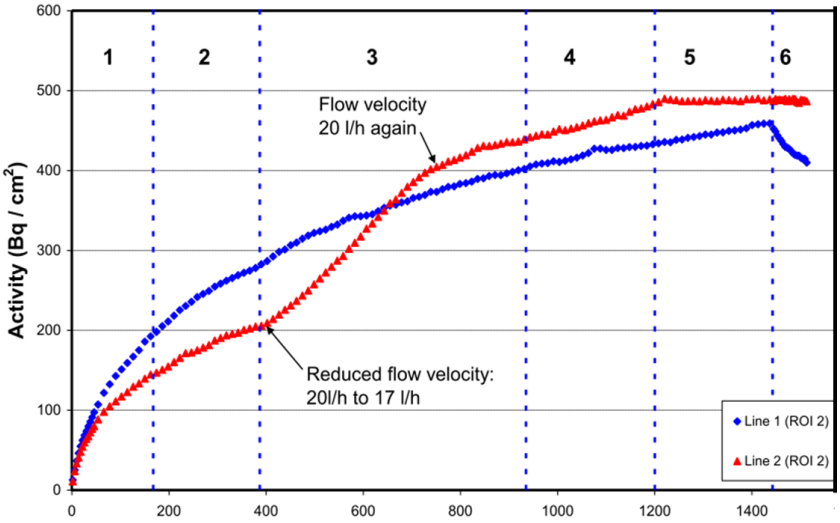

Figure 1
Activity build-up on stainless steel piping surfaces under Ni-surplus condition (line 2) and without Ni or Fe injection (line 1) [2].

Table 1
Additions of ions to K104:2 part 1, Figure 1.

Sequence No	**Start time (h)**	**Chemistry**			
		Line 1 [Co]* (ppb)	**[Fe^{3+}]/[Ni^{2+}] (ppb)**	**Line 2 [Co]* (ppb)**	**[Fe^{3+}]/[Ni^{2+}] (ppb)**
1	0	0.1	-	0.1	-
2	168	0.1	0.1/0.2	0.1	0/0.2
3	387	0.1	0.1/0.2	0.1	0/2
4	935	0.1	0.1/0.2	0.1	0.1/2
5	1200	0.1	0.1/0.2	0.1	0.1/10
6	1443	-	0.1/0.2	-	0.1/10

*marked with 60 Bq/l Co-60

A reduced flow of water from 20 l/h to 17 l/h has the following consequences for the experiment:

i. Decreases the linear flow velocity at the sample from 0.6 to 0.5 m/s.

ii. Increases the concentration of ions in the bulk water since the injection rate of ions (Fe, Co, Ni) to the system is constant.

To quantify the effect of the reduced flow velocity for the activity build-up the slopes of the curves, which correspond to the rates for activity build-up (Bq/cm^{2}h), are calculated and presented in Figure 2 and Table 2. Data according to the reduced flow velocity is presented in the following section. The flow is reduced from about t~390 h to t~740 h.

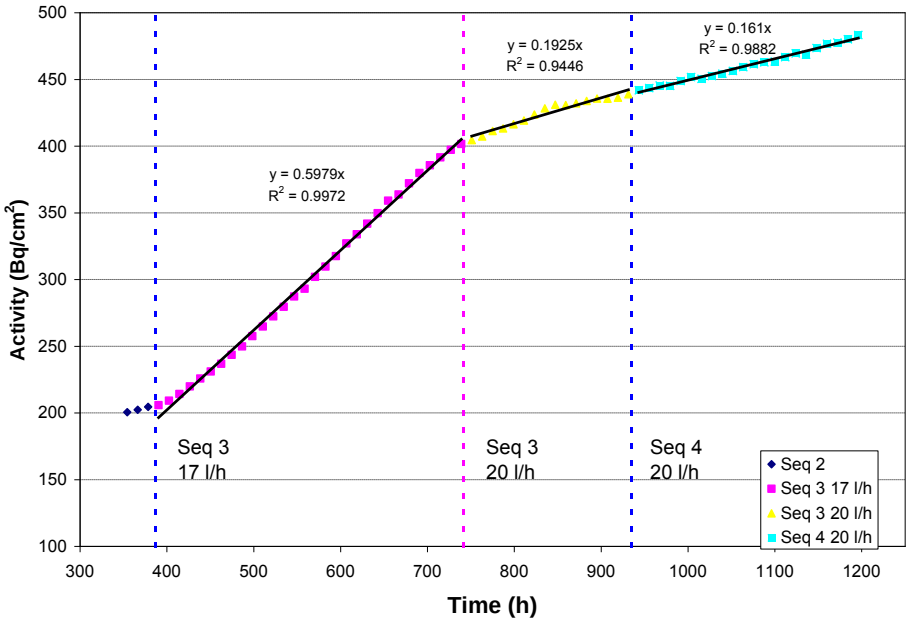

Figure 2
Activity build-up for sequence 3 and 4 with calculated slopes, rate for activity build-up (Bq/cm^{2}h), for the different flow velocities. The flow is reduced from about t~390 h to t~740 h.

Table 2
Rates for activity build-up (Bq/cm^{2}h) for sequence 3 and 4. In this table the intended concentrations of Ni and Fe is presented, not the concentrations as a result of the reduced flow velocity. The increased concentrations, as result of the reduced flow velocity will be presented in the following.

Sequence	**Flow velocity (l/h)**	**[Ni] + [Fe] (ppb)**	**Rate of activity build-up (Bq/cm^{2}h)**
2/3	20	0.2	0.4
3	17	2	0.6
3	20	2	0.2
4	20	2 + 0.1	0.2

Evaluating the effect of the reduced flow velocity upon activity build-up Sequence 4 is comparable to sequence 3 since the chemistry is similar; the difference is that also 0.1 ppb Fe is added to sequence 4. The rates for activity build-up are moreover identical for Sequence 3 and 4, 0.2 Bq/cm^{2}h. Comparing the rates of activity build-up in Table 2 it can be seen that the rate for activity build-up increases from 0.2 Bq/cm^{2}h to 0.6 Bq/cm^{2}h as the flow velocity of the water is reduced from 20 l/h to 17 l/h. The activity build-up is increased by a factor of three, which is 300 %.

The increase in ion concentration due to reduced total flow of water is now further analyzed. In this test, the volume of added Ni and Co was monitored by their weight injected. From the weight loss of the prepared solution a dosage flow (ml/min) was calculated. This was done since the pumps (HPLC) could be unstable[1]. In Figure 3 the injection rate of nickel solution given by the pump and activity build-up versus time is shown. The *injection rate* of Ni is not affected by the reduced flow velocity however the resulting *concentration* of Ni is (since it is dependent upon the main flow). Sequence 3 is shown between the blue vertical lines. From the first blue line to the pink vertical line the flow of water is 17 l/h, after the pink vertical line the flow is 20 l/h. From Figure 3 it can be seen that the injection rate of nickel solution given by the pump is increased in the beginning of sequence 3. This is due to instability of the nickel injection pump[1] and not a result of the reduced flow velocity. The variation in injection rate of nickel solution is reflected in the conductivity measured at the loop outlet, as shown in Figure 4. As can be seen in Figure 4, the conductivity increases as the increased injection rate of nickel solution is increased. At the time 740 h, however, a dip in conductivity is seen which is not seen in the injection rate of the nickel solution. This dip corresponds to the return to the normal flow rate of water to 20 l/h. This lowers the concentration of the injected ions and therefore also the conductivity.

The activity build-up and conductivity measured at the outlet vs time is shown in Figure 5. The conductivity and activity build-up are increased as a consequence of the reduced flow velocity.

[1] In the following work (from K104:2 part 2) an improvement in the experimental set-up has been implemented and the pump flow is now regulated on the weight change. A more accurate injection of ions has been achieved.

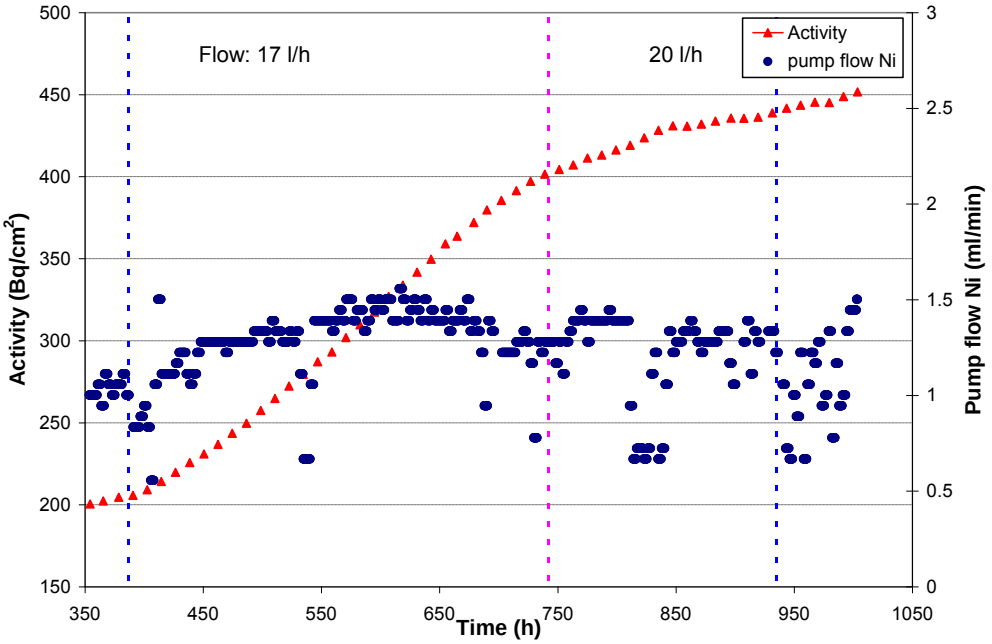

Figure 3
Time dependence of activity build-up (left y-axis) and injection rate of nickel solution (right y-axis) for sequence 3 of the test K104:2 part 1.

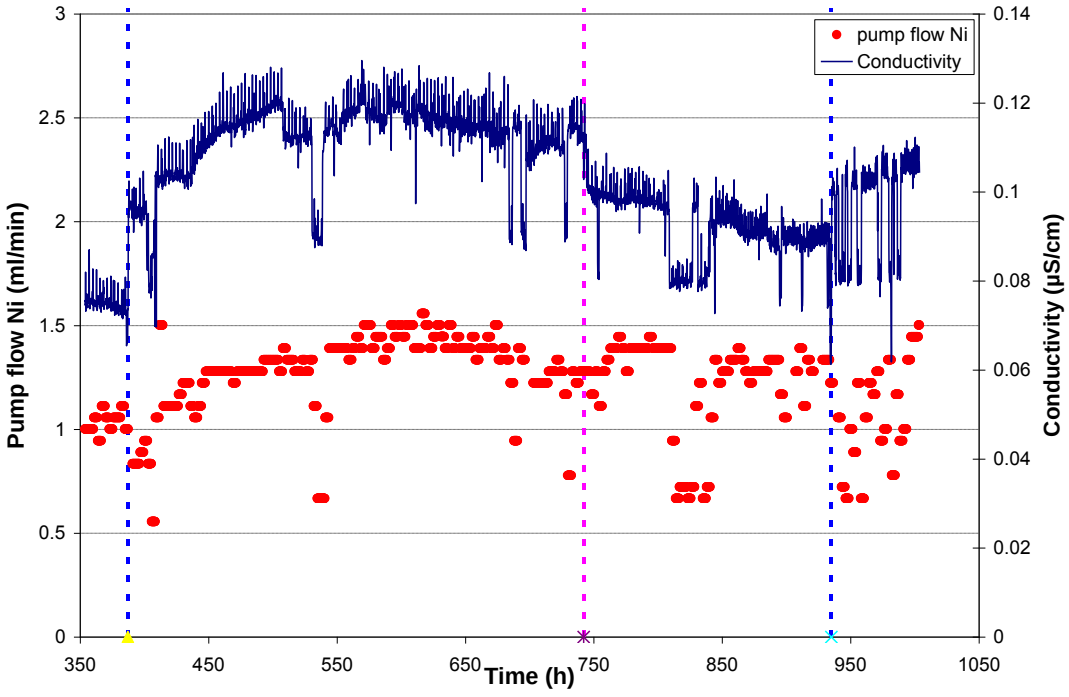

Figure 4
Time dependence of flow rate of nickel solution (left y-axis) and conductivity measured at the outlet (right y-axis) for sequence 3 of the test K104:2 part 1.

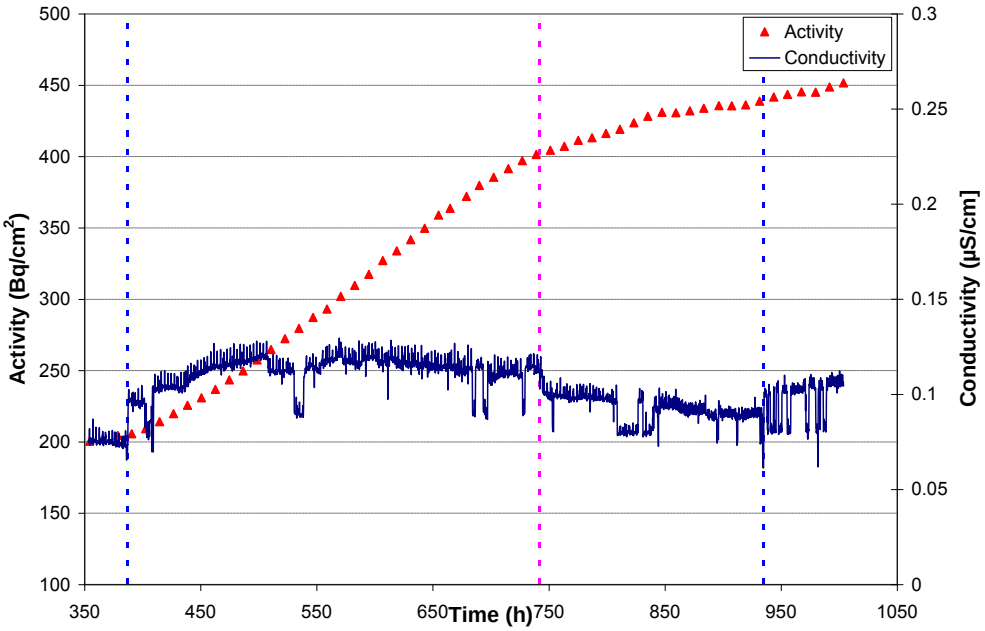

Figure 5
Time dependence of activity build-up (left y-axis) and conductivity measured at the outlet (right y-axis) for sequence 3 of the test K104:2 part 1.

The resulting bulk concentrations of Ni and Co and injected activity of Co-60, respectively, due to the reduced flow velocity is calculated from the respective injection rates and flow of water. The results are presented in Figures 6-8 respectively. An increase in bulk Co concentration is seen as the flow velocity is reduced, ~10% (Figure 7). In Figure 8 the injected activity of Co-60 is given for the time period of reduced flow velocity. The reduced flow velocity increases the concentration of Co-60 from ~66 Bq/ l to ~73 Bq/l, which also corresponds to ~10 %.

The resulting bulk concentration of Ni due to the reduced flow velocity is shown in Figure 6 and 9 (blue line in Figure 9). The pink line in Figure 9 corresponds to the concentration of Ni as it should have been if the flow rate should have been normal. From Figure 9 it can be seen that the concentration of Ni increases from ~2 ppb to ~3.5 ppb for the time period of reduced flow rate. The highest concentration is seen around 600 h, after that the concentration of Ni decreases again to ~2.5 ppb. The concentration of Ni is 2.5 ppb as the water flow is returned to 20 l/h again.

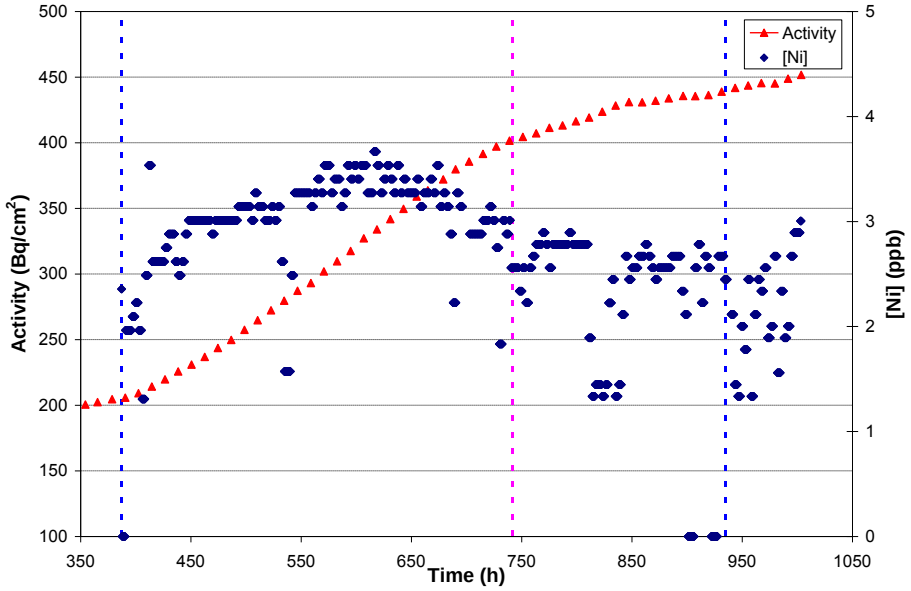

Figure 6
Activity build-up (left y-axis) and calculated concentration of Ni where the reduced flow rate has been considered (right y-axis) vs time for sequence 3, K104:2 part 1.

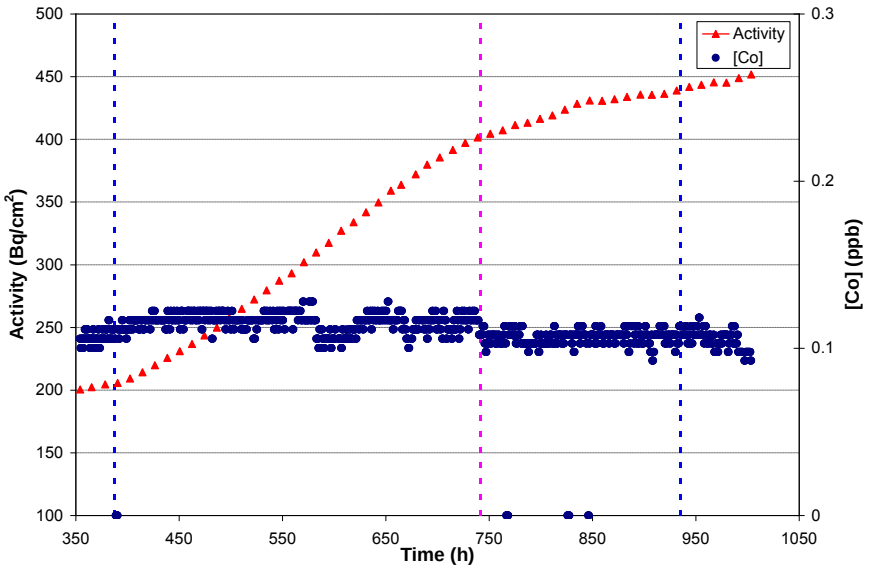

Figure 7
Activity build-up (left y-axis) and calculated concentration of Co (right y-axis) where the reduced flow rate has been considered vs time for sequence 3, K104:2 part 1.

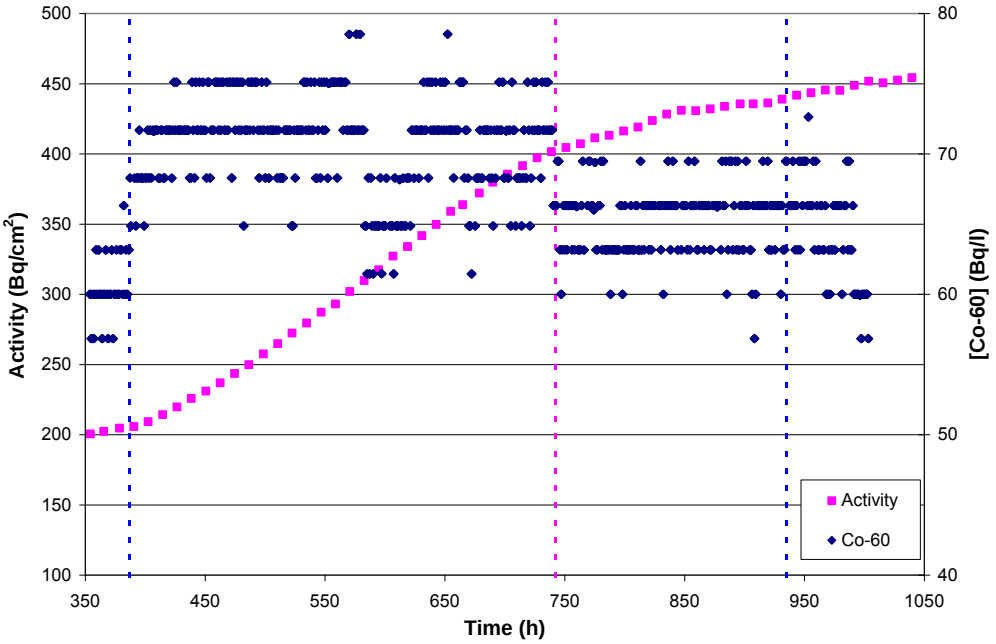

Figure 8
Activity build-up (left y-axis) and concentration of Co-60 (right y-axis) vs time for sequence 3, K104:2 part 1.

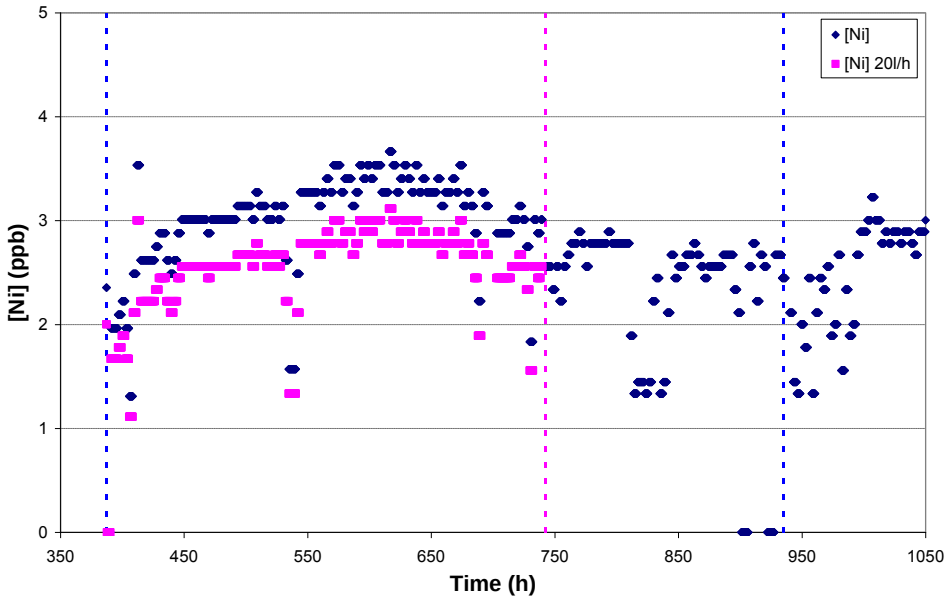

Figure 9
Concentration of Ni compensated (blue) and not compensated (pink) for the reduced flow rate of water for sequence 3 and 4, K104:2 part 1.

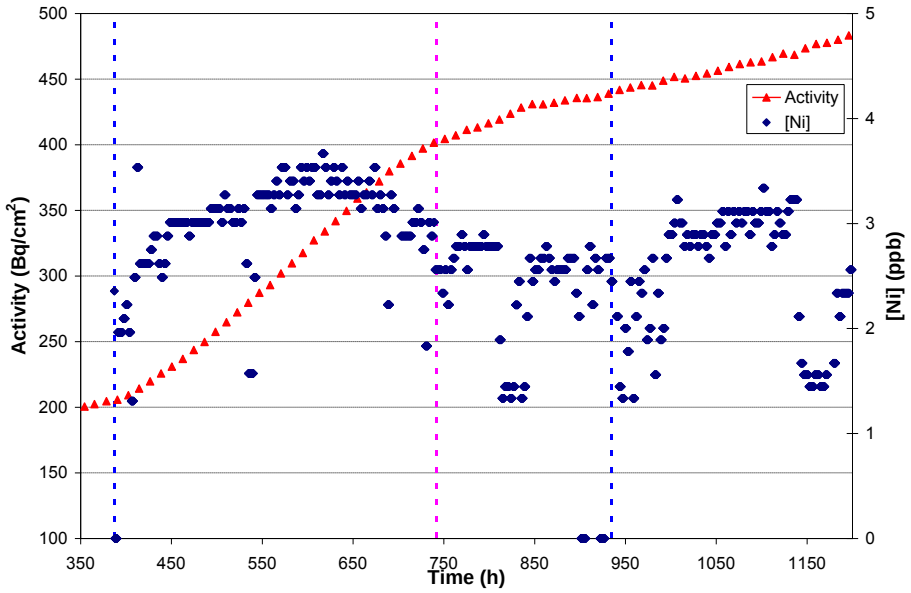

Figure 10
Activity build-up (left y-axis) and concentration of Ni (right y-axis) vs time for sequence 3 and 4, K104:2 part 1.

In Figure 10 also the activity build-up and bulk Ni concentration for sequence 4 is shown. A similar increase in Ni concentration is seen in sequence 4 (from ~2 ppb to ~3 ppb) as in sequence 3. In sequence 4 the activity build-up is however not affected by the increased bulk Ni concentration. This observation indicates that it is not mainly the bulk Ni concentration that causes the pronounced effect of increased activity build-up during the reduced flow velocity in the beginning of sequence 3. Increased Ni bulk concentration is moreover known to decrease the rate for activity build-up (and not increase) according to literature [16].

In summary, evaluation of data indicates that the increase in bulk Ni concentration, from ~2 ppb to ~3 ppb, due to the reduced main flow most likely not is responsible for the increased rate for activity build-up. The Co concentration is increased 10 % due to the reduced main flow. Any conclusion upon the influence of the 10 % increase in Co-concentration upon activity build-up could not be drawn from this data.

1.2 Influence of ion/corrosion products

In this section of the report a detailed analysis on the influence of different ions/corrosion products upon the activity build-up is given.

1.2.1 Experimental observations

To evaluate the effect of additions of different ions and concentrations upon activity build-up, the Co-deposition rates for different chemistries is calculated. In the experiments inactive Co (0.1 ppb) marked with Co-60 was added to the water. From the specific activity, Bq Co-60 per gram Co, the amount of deposited Co could be calculated. The deposited amount of Co (µmol/m^2) is shown on the y-axis and time (h) on x-axis in Figures 11-14 presented below. The Co-deposition rate in µmol/m^2h is calculated from this data. The results from the calculations are presented as shown in Table 3. Activity release to the water as the Co-addition to the water is stopped is studied in all experiments for the last sequence and will be discussed separately in the report.

Table 3
Summary of Figures and Tables for calculated Co-deposition rates for different experiments.

Experiment	Co-deposition (µmol/m^2h)	
	Figure No.	Table No.
K104:2 part 1	13	7
K104:2 part 2	14	8
K104:3	15	9
K104:4	16	10

In Figure 11 and Table 4 the results from K104:2 part 1, where the influence of Ni injection to the water on activity build-up was studied, are presented. In Figure 19 the results from all studies are summarized to get an overview of trends of different ions and concentrations in the water on activity build-up.

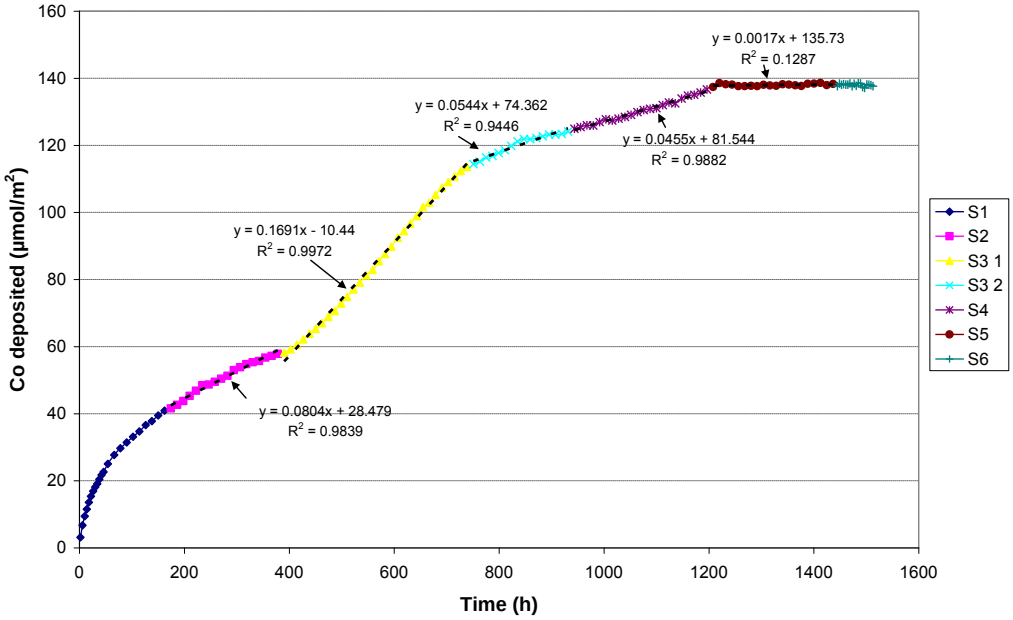

Figure 11
Co deposition, calculated from the ratio of inactive to active Co added to the water, vs time for different chemistries (S1- S6) as presented in Table 4 for K104:2 part 1, line 2.

Table 4
Rates for Co-deposition in K104:2 part 1 line 2.

Sequence No.	Chemistry [Fe]/[Ni] (ppb)	Co-deposition rate[2] (µmol/m^{2}h)	R^2-value linear regression
1	-	-	-
2	0/0.2	0.08	0.9839
3 part 1	0/2	0.17 (0.14*)	0.9972
3 part 2	0/2	0.05	0.9446
4	0.1/2	0.05	0.9882
5	0.1/10	0.01	0.1287
6 (release)	0.1/10	-	-

*Re-calculated Co-deposition rate for the reduced flow velocity that causes another ratio of active to inactive concentration of Co.

[2] *The calculated values are based on the assumption that the rates are constant over the periods of exposure. Normally the rate decreases with time for longer exposures [9]. The data could however be used for comparing trends for activity build-up for different concentrations of ions.*

In Figure 12 and Table 5 the results from K104:2 part 2, where the influence of Fe injection to the water on activity build-up was studied, are presented [2]. In Figure 19 the results from all studies are summarized to get an overview of trends of different ions and concentrations in the water on activity build-up.

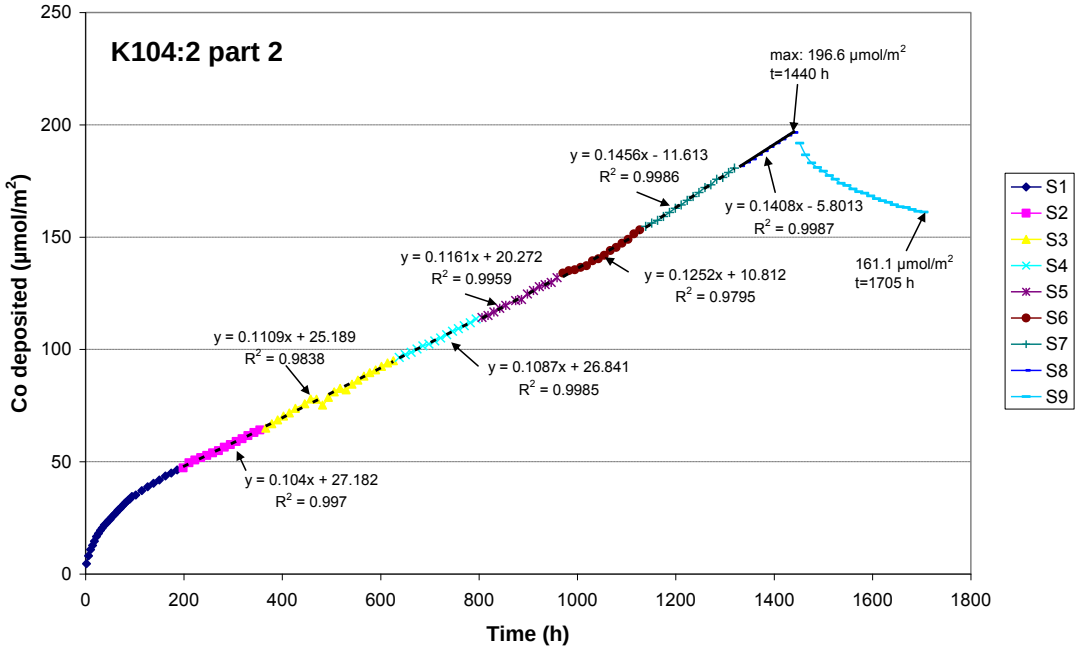

Figure 12
Time dependence of Co deposition, calculated from the ratio of inactive to active Co added to the water for different chemistries (S1- S9) as presented in Table 5 for K104:2 part 2, line 2.

Table 5
Rates for Co-deposition in K104:2 part 2 line 2.

Sequence No.	Chemistry [Fe] (ppb)	Co-deposition rate (µmol/m^{2}h)	R^2-value linear regression
1	-	-	-
2	0.1	0.10	0.997
3	0.5	0.11	0.9838
4	1	0.11	0.9985
5	2	0.12	0.9959
6	5	0.13	0.9795
7	10	0.15	0.9986
8	15	0.14	0.9987
9 (release)	15	-	-

In Figure 13 and Table 6 the results from K104:3, where the influence of different ratios of [Fe] to [Ni] in the water on activity build-up was studied are presented. In Figure 19 the results from all studies, are summarized to get an overview of trends of different ions and concentrations in the water on activity build-up.

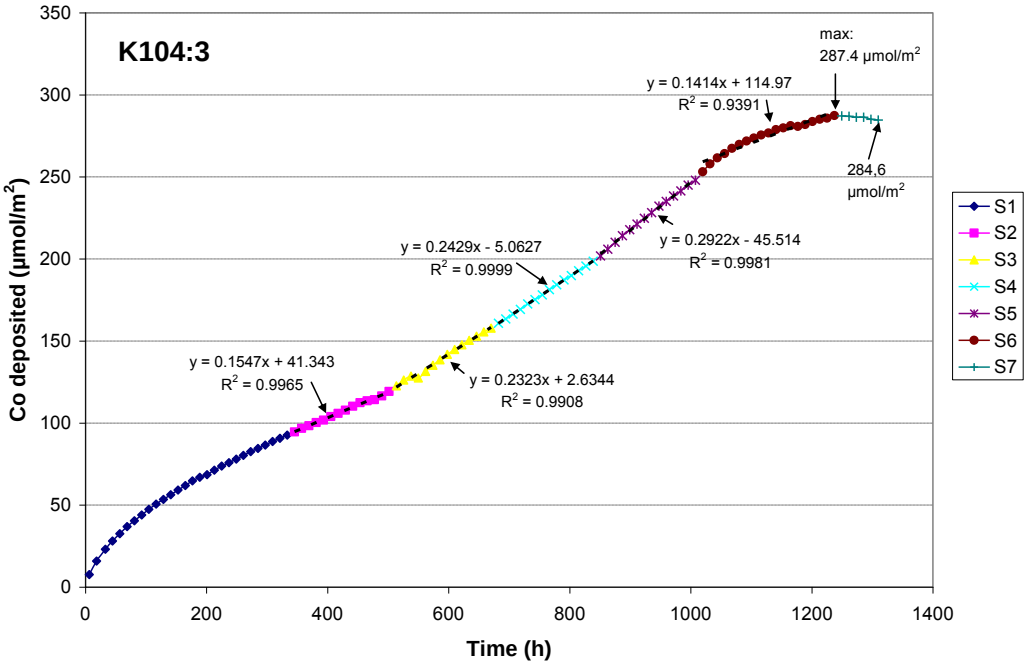

Figure 13
Co deposition, calculated from the ratio of inactive to active Co added to the water, vs time for different chemistries (S1- S7) as presented in Table 6 for K104:3, line 2.

Table 6
Rates for Co-deposition in K104:3 line 2.

Sequence No.	Chemistry [Fe]/[Ni] (ppb)	Co-deposition rate (µmol/m^{2}h)	R^2-value linear regression
1	-	-	-
2	2/0	0.15	0.9965
3	2/0.5	0.23	0.9908
4	2/1	0.24	0.9999
5	2/5	0.29	0.9981
6	2/10	0.14	0.9391
7 (release)	2/10	-	-

In Figure 14 and Table 7 the results from K104:4 where the influence of different ratios of [Fe] to [Zn] to the water on activity build-up was studied are presented [4]. In Figure 19 the results from all studies are summarized to get an overview of trends of different ions and concentrations in the water on activity build-up.

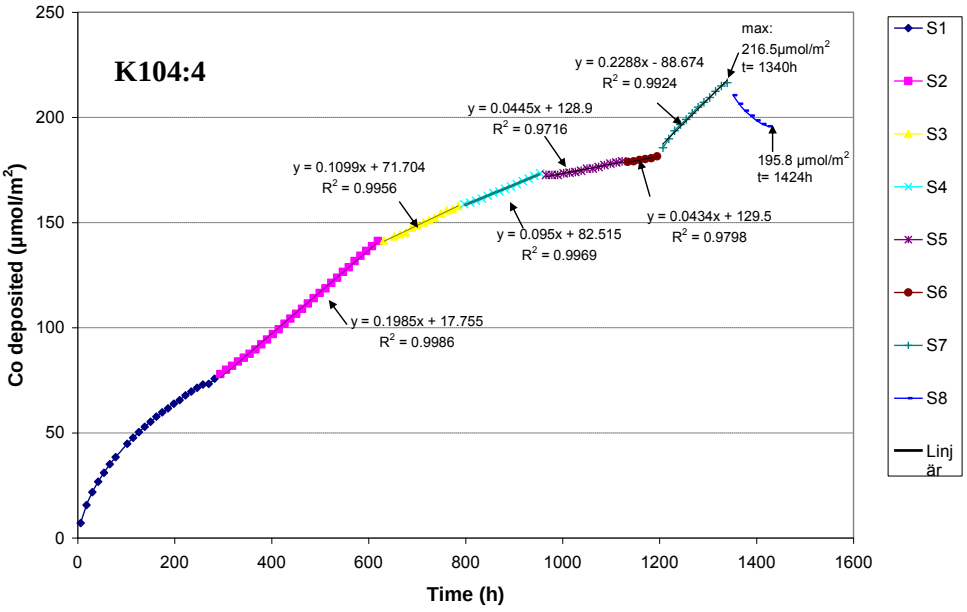

Figure 14
Co deposition, calculated from the ratio of inactive to active Co added to the water, vs time for different chemistries (S1- S8) as presented in Table 7 for K104:4, line 2.

Table 7
Rates for Co-deposition in K104:4 line 2.

Sequence No.	Chemistry [Fe]/[Zn] (ppb)	Co-deposition rate (µmol/m2h)	R2-value linear regression
1	-	-	-
2	2/0	0.20	0.9986
3	2/0.5	0.11	0.9956
4	2/1	0.10	0.9969
5	2/5	0.04	0.9716
6	2/10	0.04	0.9798
7	2/0	0.23	0.9924
8 (release)	2/0	-	-

In all experiments the activity build-up was also studied in a separate line, line 1, where only 0.1 ppb Co marked with Co-60 was added to the water. In experiment K104:2, part 1, also 0.2 ppb Ni and 0.1 ppb Fe were added to the water. The Co-deposition rates have also been calculated for the experiments in line 1 and are presented in Figures 15-18 and summarized in Table 8.

In Figure 15 the Co-deposition in line 1 for experiment K104:2 part 1 is shown. The Co-deposition rate is tabulated in Table 11.

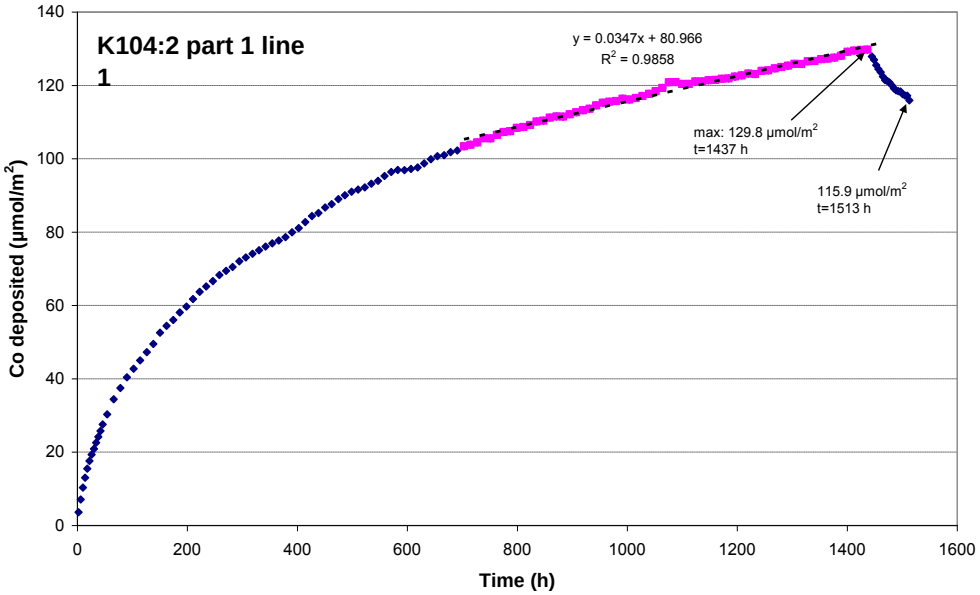

Figure 15
Co deposition, calculated from the ratio of inactive to active Co added to the water, vs time for line 1, K104:2 part 1.

In Figure 16 the Co-deposition in line 1 for experiment K104:2 part 2 is shown. The Co-deposition rate is tabulated in Table 8.

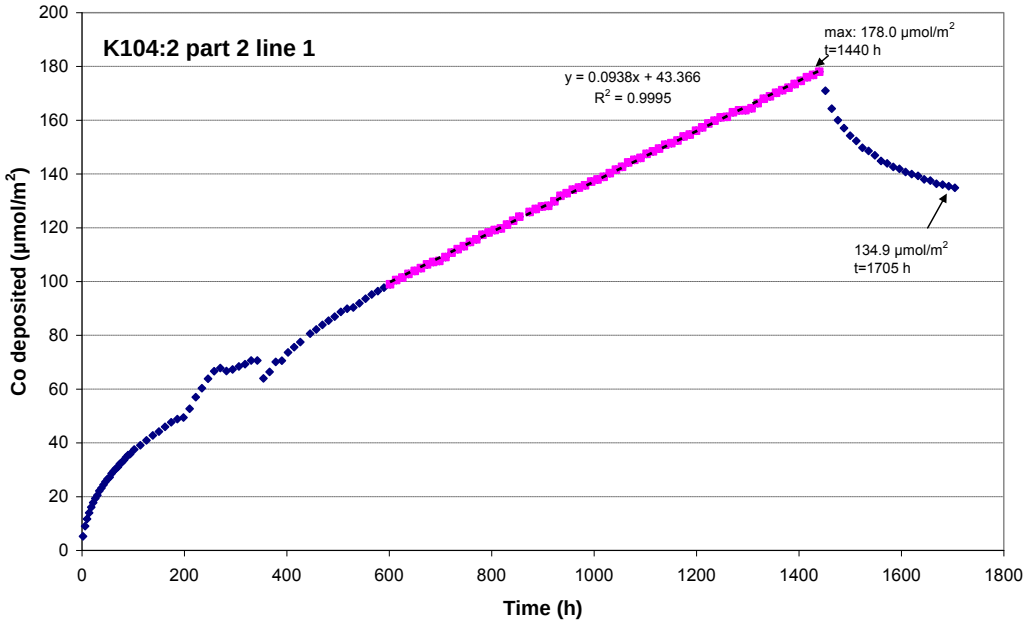

Figure 16
Co deposition, calculated from the ratio of inactive to active Co added to the water, vs time for line 1, K104:2 part 2.

In Figure 17 the Co-deposition in line 1 for experiment K104:3 is shown. The Co-deposition rate is tabulated in Table 8.

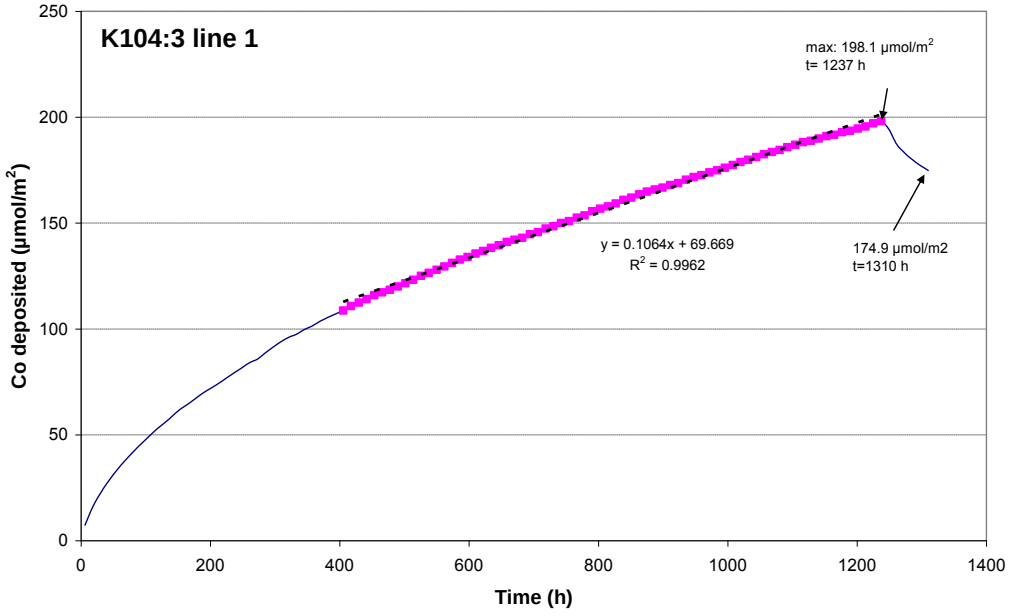

Figure 17
Co deposition, calculated from the ratio of inactive to active Co added to the water, vs time for line 1, K104:3.

In Figure 18 the Co-deposition in line 1 for experiment K104:4 is shown. The Co-deposition rate is tabulated in Table 8. At t ~750 h the Co-addition to line 1 was unplanned stopped which resulted in an immediate release of Co to the water. At t ~ 800 h, the Co-addition was started again. Activity release to the water as the Co-addition to the water is stopped is discussed separately in next chapter of the report.

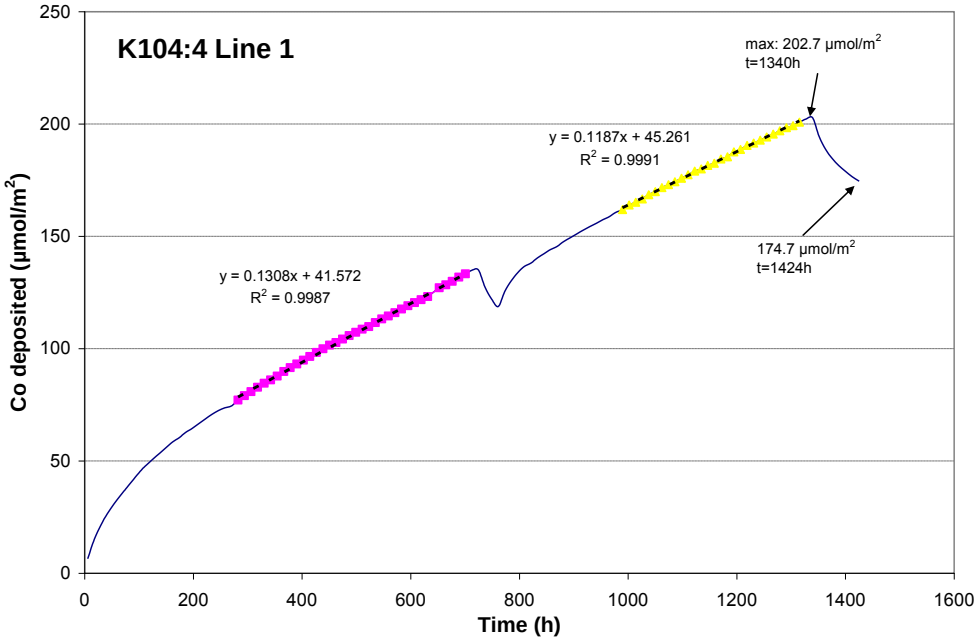

Figure 18
Co deposition, calculated from the ratio of inactive to active Co added to the water, vs time for line 1, K104:4.

Table 8
Rates for Co-deposition in line 1. 0.1 ppb Co marked with Co-60 was added to the water.

Experiment	Rate Co-dep (µmol/m^{2}h)	R^2-value
K104:2 part 1*	0.03	0.9858
K104:2 part 2	0.09	0.9995
K104:3	0.11	0.9962
K104:4 a	0.13	0.9987
K104:4 b	0.12	0.9991

*In experiment K104:2, part 1, also 0.2 ppb Ni and 0.1 ppb Fe were added to the water.

Figure 19 shows the maximum deposited Co in at % in the oxides formed in different tests in K104 project. Assuming a constant Co-deposition rate of 0.1 μmol m^{-2} h^{-1} for an exposure period of 1500 h, the total atomic fraction of Co would be approx. 0.15 at % in a $NiFe_2O_4$ layer of 0.6 μm.
The Co deposited in line 1 is comparable since the chemistry (addition of ions) is identical (except K104:2 part 1) throughout the experimental series. From Figure 19 it could be seen that the reproducibility in line 1 is improved as the experimental system is optimized in experiments K104:3 and K104:4.

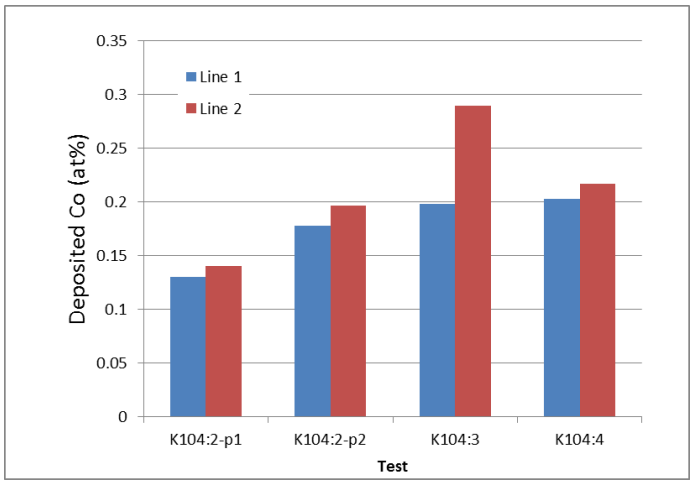

Figure 19
Maximum deposited Co (in at %) in oxides in different tests.

1.3 Activity release studies

In this section of the report data Co-release data obtained from the experiments is further analyzed. The purpose is to receive more information about important processes for the activity build-up occurring at the oxide-water interface.

In the activity release studies the release of activity is followed as the Co injection to the water was stopped. During the release studies the injection of other metal cations from previous sequence was kept unchanged. Release studies were done for all tests in the last sequence of the experiments. In this chapter the activity release studies for all experiments are further evaluated and discussed according to the following mechanisms for the observed activity release:

- Renewable of the surface oxides due to precipitation and dissolution.
- Activity uptake and release due to oxide growth and oxide renewal.
- Fast activity build-up and release due to diffusion through the porous inner oxide layer.
- Desorption of adsorbed Co at the surface.

1.3.1 Experimental observations

In Figure 20 all release studies performed in the experimental series are summarized. The data have been normalized regarding both time and Co deposition to facilitate evaluation. Normalization has been done to be able to evaluated differences in the initial activity release which is much easier if the curves are superimposed on each other. The curves to the left of the vertical line in the figure show the activity build-up at different chemistries (as indicated in the figure) as Co is still added to the water. To the right of the vertical line Co addition to the water is stopped and the chemistry from the sequence before is kept (with one exception for K104:2 part 2 where the Fe concentration before Co stop is 15 ppb and after 5 ppb). The figure shows the change of Co content at the sample as Co addition to the water is stopped.

The following observations are made:

- The release of Co is the lowest at a mixed injection of 10 ppb Ni and 0.1 ppb Fe.
- The release of Co is the highest when no injection of Fe and Ni (pure water) is applied.
- The release of Co is relatively low when injection of Fe (2 and 5 ppb) is applied compared to that without injection of Fe(pure water).
- The release of Co is relatively low when injection of a mixed Fe (0.1 ppb) and Ni (0.2 ppb), compared to that without injection of both (pure water).

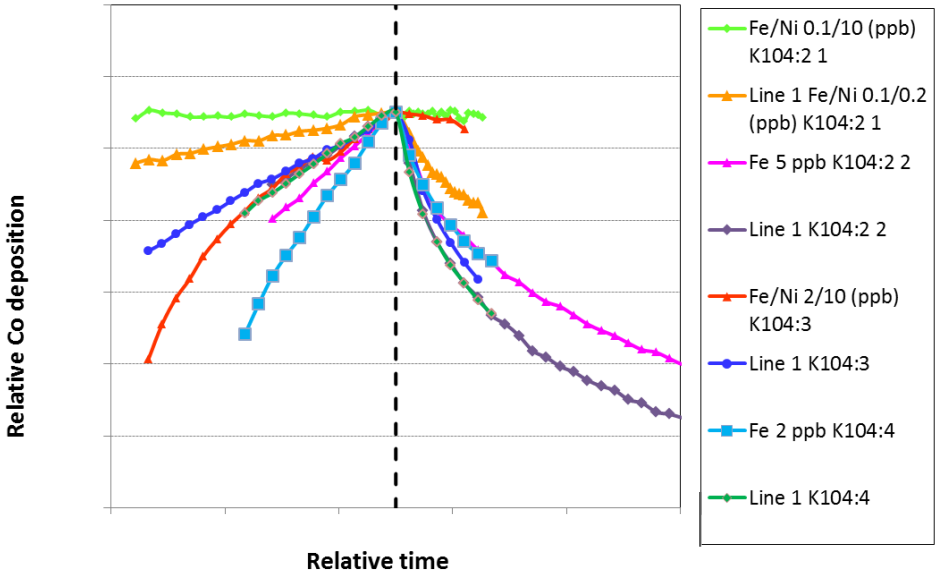

Figure 20
Release studies in all experiments on relative y- and x-axis. At the black vertical dotted line the addition of Co to the water is stopped but the addition of other ions is kept (indicated in the figure).

1.3.2 Discussion

In the release studies the activity release on the test section surfaces was measured as no Co was added to the water. In this section of the report different processes at the surface that may be responsible for the change in Co measured by the gamma detector during the release studies will be discussed (1-4 below). Firstly, an assumption is made where the activity release is correlated to dissolution of the oxide in contact with water (1), secondly two alternatives from a previous work [7] for interpretation is discussed (2-3). Lastly, a discussion is given where the activity release is correlated to desorption of adsorbed Co at the surface. The discussions given in the report are however preliminary and needs further validation, which is beyond the scope of this work.

1. Renewable of the surface oxides due to precipitation and dissolution.
2. Activity uptake and release due to oxide growth and oxide renewal.
3. Fast activity build-up and release due to diffusion through the porous inner oxide layer.
4. Desorption of adsorbed Co at the surface.

1. Renewable of the surface oxides due to precipitation and dissolution

Firstly, the observed activity release is correlated to renewable of surface oxide in contact with water through precipitation and dissolution reactions by calculating a dissolution rate of $NiFe_2O_4$ from the data. In the calculations all oxides are assumed to be $NiFe_2O_4$ and Co is assumed to occupy 1/100 of the metal sites, which corresponds to 0.4 at % Co (a slightly higher Co-content close to the water is assumed in the calculation). In the calculation a linear release of Co and constant $NiFe_2O_4$ composition is assumed (which of course is a simplification). A slightly increased surface area (2.5) due to surface roughness is also assumed in the calculations. Release data from time period of 70 -80 h is used in the calculations.

On average, a $NiFe_2O_4$ dissolution rate in the size of 10^{-10} kg/m^{2}s is calculated. This number is similar to the value measured [10] at 80 - 250 ºC (3-9 x 10^{-9} kg/m^{2}s). Since there is no $NiFe_2O_4$ dissolution rate measured at 280 ºC a direct comparison between the estimated value and measured value is not possible. The calculated dissolution rate of $NiFe_2O_4$ (10^{-10} kg/m^{2}s) could be correlated to the corrosion rate of stainless steel. Correlating the calculated dissolution rate of $NiFe_2O_4$ to the corrosion rate of stainless steel 316L gives a corrosion rate of 1 µm/ year. The calculated metal corrosion rate of 1 µm/year agrees well with assumed corrosion rates for stainless steel in BWR environments. Therefore the precipitation and dissolution of $NiFe_2O_4$ in the oxide/water interface could be assumed to be of importance for the observed Co-release measured in the release studies. The satisfying correlation of dissolution data with corrosion rate of stainless steel also indicates that the *solubility of the oxide in contact with water* is crucial for the corrosion of stainless steel in high temperature water.

2. Activity uptake and release due to oxide growth and oxide renewal

The activity uptake and release due to oxide growth and oxide renewal was discussed in a previous report [7]. According to the calculations performed in *1)* the corrosion rate of stainless steel could be correlated to the activity release. According to the calculations performed above, the corrosion rate of stainless steel in turn seems to be dependent upon the stability of the oxide in contact with the water.

The Co-60 release rate and initial Co-60 build-up rates were compared in the previous work [5]. One can see that both rates are similar (Figure 21) and both decrease with time linearly. Suppose the return rate is correlated to oxide dissolution according to the calculations performed in *1)*. Oxide containing Co is dissolved to the water. This is measured as an activity release at the sample. The activity measured in the release studies at the sample is the net result of the precipitation and dissolution reactions. Similarly the activity measured during the initial activity build-up could be the net result of the precipitation and dissolution reactions - therefore the rates for activity build-up and activity release could be similar as shown in Figure 21. The measured rates are the result of the same process - precipitation and dissolution - therefore they are similar.

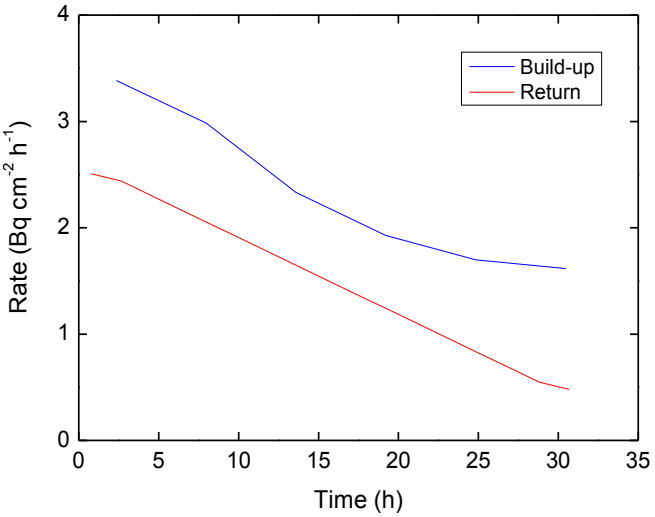

Figure 21
The rates of initial activity build-up and activity return. Re-calculated from Ref. [16].

Followed a discussion is given which provides one example of interpretation of the shape of the activity build-up curves in the experiments. The typical shape of activity build-up in these experiments is presented in all line 1 experiments. Activity build-up proceeds with a higher rate initially resulting in a sharp curve. The rate is then decreased and the activity build-up curve is flattening out, however it still increases slightly. Assume a certain *amount* of oxide (“thickness”) in contact with water is continuously renewed through

precipitation and dissolution. The Co-content in this *amount* of oxide is constant for stable water chemistry conditions. The Co-atoms in this *amount* of oxide will however diffuse into the oxide. The slight increase in activity build-up (after the initial shaper increase) could be a consequence of diffusion of Co atoms into the oxide. The Co-content in the *amount* of oxide in contact with water is only constant for stable ("constant") water chemistry conditions. Upon changes in water chemistry conditions, for example going from no Co in the water (during the pre-oxidation) to start of the experiments where Co is injected and similarly but reversed as the Co concentration in the water is stopped (activity release study), the Co-concentration in this *amount* of oxide is not constant but changed. The change in Co-concentration in this *amount* of oxide initially and in the release study could be an explanation for the high rates measured initially during activity build-up and during the activity release studies.

3. Fast activity build-up and release due to diffusion through the porous inner oxide layer

This mechanism presents another way of interpretation of the high activity build-up rate in the beginning of an exposure test and the sharp activity drop when Co(II) injection was stopped. Consider that diffusion in a solid oxide grain is an extremely slow process. It is unlikely that approximately 10 % of total activity of the tube section returned within 30 h through such a diffusion process alone. An easier path would be that ^{60}Co(II) nuclides in the cavity (pores) of the inner oxide layer release into the water through diffusion via pores and much defected grain boundaries. Since the diffusion in such a medium is relatively fast, presumably in a matter of tens of hours, it could explain the relatively high return rate in the beginning of the return test. Once the concentration of Co(II) in the cavities of the inner oxide layer is decreased to the same low level as in the bulk water, the driving force for diffusion ceases to exist. However, corrosion of the inner oxide layer proceeds and its oxide get renewed, leading to further activity reduction in this layer. Eventually the inner oxide layer will contain little or no ^{60}Co(II) radionuclides. Since the inner oxide layer is approximately 1/5 of the total oxide formed a total replacement of this inner oxide layer by newly formed oxide might give an activity reduction in the similar order of magnitude as observed in the return tests. The interpretation of the return rate by this mechanism may also be used to explain the similarly fast build-up rate in the porous inner oxide layer once the pre-exposed sample is exposed to ^{60}Co(II) containing water. Diffusion of ^{60}Co(II) from the bulk water into the porous inner oxide layer would be approximately as fast as it returns from the inner oxide layer to the bulk water in a return test.

4. Desorption of adsorbed Co at the surface

Another way of interpretation is related to desorption of adsorbed Co at the surface. To get an idea if the Co that is released in the study fits on one surface layer of the oxide surface, if the released Co only is due to desorption of Co from the top surface, a rough calculation is made. In the calculation all oxides at the surface are assumed to be $NiFe_2O_4$. A deposition rate of 0.1 μmol/m^2h, will correspond to 10^{17} Co-atoms/m^2h. Two scenarios are studied.

1. All deposited Co-60 atoms are allocated on (100) plane of a $NiFe_2O_4$ crystal.
2. All deposited Co-60 atoms are homogenously allocated in a $NiFe_2O_4$ layer of 0.6 μm.

Case 2 has been already treated in Section 3.2.1. It shows that 0.1 μmol/m^2 corresponds to a Co-concentration of approx. 0.15 at % in a layer of $NiFe_2O_4$ of 0.6 μm.

An illustration is made upon how many Co-atoms would sit on a $NiFe_2O_4$ grain if all deposited Co-atoms are adsorbed on surface. Consider the surface of a $NiFe_2O_4$ crystal cell. One-side area of a cell is thus 70.73 $Å^2$. Consider a Co-deposition of 200 μmol/m^2, if all Co-atoms should be allocated on spinel surface only (no Co-atom inside oxides) there will be approximately 85 Co-atoms appeared. They are simply too many for the surface to allocate. For a typically amount of 30 μmol/m^2 in a release test, it is equivalent to 13 Co-atoms per cell surface which release. This number is still too large to be allocated on a cell surface. However, if these Co-atoms are allocated in the entire oxide layer, the average Co fraction is approx. 0.2 at %. The released amount is thus approx. 10 % of total. In other words, the released Co atoms must have largely come from the Co-atoms that have already been incorporated in the oxide layer. From microstructure evaluations however, (next chapter in the report) it has been seen that the inner oxide is extensively porous. Adsorption of Co on oxide surfaces in the pores increases the number of available sites for Co which makes desorption of Co still as an alternative for the observed Co-release.

1.3.3 Summary

Evaluation of activity release data show that the activity release could be correlated to the dissolution rate of the oxide in contact with the water. This indicates that the precipitation and dissolution reactions continuously going on in the oxide-water interface could be of importance for the activity build-up. The calculated dissolution rate could moreover be correlated to the corrosion rate for stainless steel in BWR environments. This indicates that the corrosion rate for stainless steel in BWR environments could be controlled by the stability (with respect to dissolution) of the oxide in the oxide-water interface. The mechanism needs however further validation. The importance of precipitation and dissolution reactions in the oxide water interface has been pointed out through:

- The calculated value of oxide dissolution in the oxide/water interface (10^{-10} kg/m^{2}s), assuming the oxide is $NiFe_2O_4$, which could be further correlated to the corrosion rate of stainless steel (1µm/year).
- The presence of Fe and Ni that minimizes the release of Co → the presence of Fe and Ni in the water, due to injection, supress the dissolution of $NiFe_2O_4$.
- The release of Co is highest where no Fe and Ni are present in the water → No injection of Fe and Ni to the water gives the highest dissolution of $NiFe_2O_4$.

An alternative way of interpretation of the Co-release data is diffusion of Co-60 through the porous inner oxide layer.

2 References

[1] Forsberg, S. & Johansson, R. (2008). *Systemytors upptag av Co-60 i närvaro av andra metalljoner. Etapp 2 — Inverkan av nickel och järn.* Studsvik Nuclear AB, STUDSVIK/N-08-129.

[2] Lin, C. C. & Smith, F. R. (1988). *BWR Cobalt Deposition Studies: Final report*, EPRI report. EPRI, NP-5808.

[3] Forsberg, S. & Pettersson, A. (2009). *Systemytors upptag av Co-60 i närvaro av andra metalljoner. Etapp 3 — Inverkan av olika kvoter järn/nickel.* Studsvik Nuclear AB, STUDSVIK/N-09-157.

[4] Björnsson, S., Gustafsson, C. & Johansson, R. (2010). *Systemytors upptag av Co-60 i närvaro av andra metalljoner. Etapp 4 — Inverkan av olika kvoter järn/zink.* Studsvik Nuclear AB, STUDSVIK/N-10-150.

[5] Chen. J. (2009). *Understanding radioactivity up-take on system piping surfaces through laboratory deposition simulation.* Studsvik Nuclear AB, STUDSVIK/N-08/213.

[6] Chen, J. (2001). Stability of trevorite in high temperature water, a radiotracer study, Studsvik Nuclear AB, STUDSVIK/N(K)-01/022. Replace with headline

2012:02

The Swedish Radiation Safety Authority has a comprehensive responsibility to ensure that society is safe from the effects of radiation. The Authority works to achieve radiation safety in a number of areas: nuclear power, medical care as well as commercial products and services. The Authority also works to achieve protection from natural radiation and to increase the level of radiation safety internationally.

The Swedish Radiation Safety Authority works proactively and preventively to protect people and the environment from the harmful effects of radiation, now and in the future. The Authority issues regulations and supervises compliance, while also supporting research, providing training and information, and issuing advice. Often, activities involving radiation require licences issued by the Authority. The Swedish Radiation Safety Authority maintains emergency preparedness around the clock with the aim of limiting the aftermath of radiation accidents and the unintentional spreading of radioactive substances. The Authority participates in international co-operation in order to promote radiation safety and finances projects aiming to raise the level of radiation safety in certain Eastern European countries.

The Authority reports to the Ministry of the Environment and has around 270 employees with competencies in the fields of engineering, natural and behavioural sciences, law, economics and communications. We have received quality, environmental and working environment certification.

Strålsäkerhetsmyndigheten
Swedish Radiation Safety Authority

SE-171 16 Stockholm
Solna strandväg 96

Tel: +46 8 799 40 00
Fax: +46 8 799 40 10

E-mail: registrator@ssm.se
Web: stralsakerhetsmyndigheten.se